FORSCHUNGSZENTRUM JÜLICH GmbH
Institut für Kernphysik

Simulation and Correction of the Closed Orbit in the Cooler Synchrotron COSY

by

D. Dinev

Jül-2406
November 1990
ISSN 0366-0885

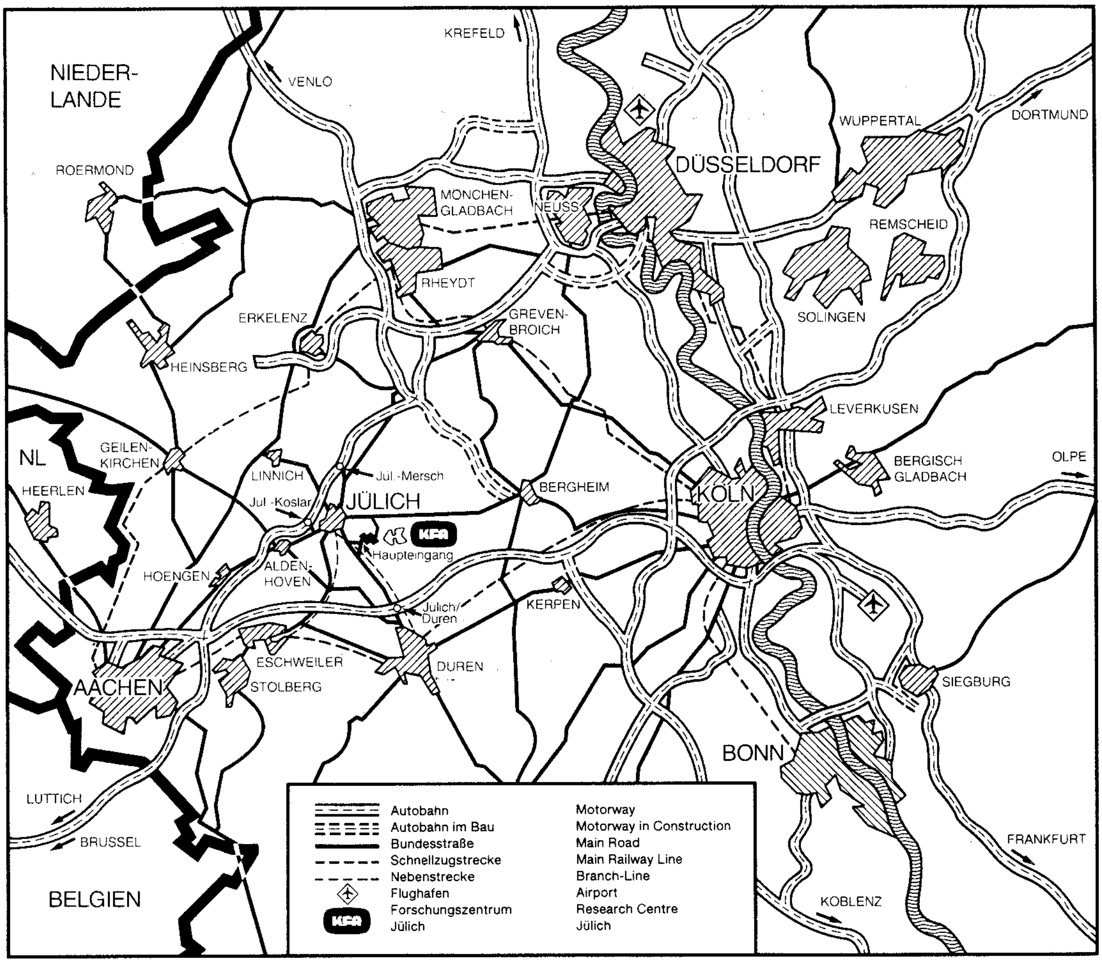

Als Manuskript gedruckt

Forschungszentrum Jülich: Berichte Nr. 2406
Institut für Kernphysik Jül-2406

Zu beziehen durch: ZENTRALBIBLIOTHEK · Forschungszentrum Jülich GmbH
Postfach 1913 · D-5170 Jülich (Bundesrepublik Deutschland)
Telefon: 02461/61-0 · Telex: 833556-70 kfad · Telefax: 02461/61-6103

Simulation and Correction of the Closed Orbit in the Cooler Synchrotron COSY

by

D. Dinev

Contents

1. Introduction

The cooler synchrotron COSY is a synchrotron and storage ring intended to accelerate protons and light ions up to an energy in the range 200 MeV—2.5 GeV.[1,2] The upgraded cyclotron **JULIC** will be used as an injector. The COSY ring consists of two 180 degree arcs and two 2π (or π) straight sections (telescopes). The arcs' magnetic structure is based on 6 FDDF (or DFFD) periods. The accelerator circumference will be 184 m. To improve the quality of the beam, both electron and stochastic cooling will be used. The maximum designed particle intensity is $2 \cdot 10^{11}$ ppp.

The main COSY parameters are listed in Appendix 1.

In this paper the problem of COSY closed orbit control and its correction is discussed. The results of a simulation of the COSY closed orbit and its correction using different correction methods are given. The interactive computer program **ORBIT**, created especially for the simulation and correction of the COSY closed orbit, is described. The paper includes as well a survey of the orbit correction methods and related topics.

2. Transverse Particle Motion under Linear Perturbations

The transverse motion of the particles in a cyclic accelerator is a superposition of a motion along a closed trajectory (equilibrium or closed orbit) and betatron and radial-phase oscillations around this curve. In a real magnetic structure both the closed orbit and the oscillations around it are distorted due to errors in the magnetic fields, displacements and tilts of the elements from their designed positions, stray fields, and ground movements. As far as the closed orbit is concerned, perturbations cause its deformation. The maximum deviation of the distorted orbit from the ideal (reference) orbit coinciding with the vacuum chamber axis reaches to some ten millimeters. Such a large deviation does not allow for the accelerator aperture to be used effectively and hampers the work of the injection and extraction systems.

This is the reason why in accelerators special systems of either small correcting magnets or additional correcting coils in the main dipoles or controlled displacements of the quadrupoles are used. These correcting systems reduce the closed orbit distortion to a sufficiently small value.

In fact correcting systems intentionally insert in the magnetic structure perturbations of the same character. The purpose of the orbit correction consists in choosing the proper strengths and positions of these intentionally inserted perturbations (corrections) so that the smallest possible deviations from the reference orbit may be achieved.

We shall begin our discussion of the closed orbit distortion and correction with a brief survey of the transverse particle motion in cyclic accelerators in the presence of so-called linear perturbations.

It is well known[3] that in the curvilinear coordinate system (s, x, y) used in cyclic accelerators where s is directed along the reference orbit, x along the main normal vector, and z along to the binormal vector, the Lagrangian of the transverse particle motion can be presented in the form:

$$\mathcal{L}(x,x',z,z',s) = p\sqrt{\left(1+\frac{x}{\rho}\right)^2+x'^2+z'^2} + e\left[\left(1+\frac{x}{\rho}\right)A_s+x'A_x+z'A_z\right] \tag{2.1}$$

In (2.1) the distance along the reference orbit s was taken to be the independent variable; ()' denotes differentiation with respect to s; p and e are the particle momentum and charge; ρ is the radius of the curvature of the reference orbit; and A_s, A_x, A_z are the vector potential components.

From (2.1) the following expression about the transverse motion Hamiltonian can be deduced:

$$\mathcal{H}(x,p_x,z,p_z,s) = -\left(1+\frac{x}{\rho}\right)\sqrt{p^2-(p_x-eA_x)^2 - (p_z-eA_z)^2} - e\left(1+\frac{x}{\rho}\right)A_s \tag{2.2}$$

We shall consider here the cases of a sector magnetic field and of a quadrupole field, which are the most important for particle accelerators. For these cases substituting in (2.2) the relevant expressions for the vector potential A and expanding the kinematical part in a power series, retaining only the major first few members one can obtain that:

$$\mathcal{H} \approx \mathcal{H}_0 = \begin{cases} \dfrac{1}{2}\dfrac{p_x^2}{p_0} + \dfrac{1}{2}\dfrac{p_z^2}{p_o} + p_o\dfrac{(1-n)}{2}\left(\dfrac{x}{\rho}\right)^2 + p_o\dfrac{n}{2}\left(\dfrac{z}{\rho}\right)^2 & \text{for a sector magnetic field} \\ \dfrac{1}{2}\dfrac{p_x^2}{p_0} + \dfrac{1}{2}\dfrac{p_z^2}{p_o} - \dfrac{eg}{2}(x^2-z^2) & \text{for a quadrupole field} \end{cases} \tag{2.3}$$

In (2.3) we denoted with $\mathcal{H}_0$ the Hamiltonian of the linearized transverse motion; $p_o = -eB_o\rho$ is the particle momentum corresponding to the reference trajectory; $B_o\rho$ is the beam rigidity; $n = -(\rho/B_o)(\partial B/\partial x)$ is the field index; and g is the quadrupole gradient.

We shall consider in this paper correcting magnets as short magnets, with small ($B_c << B_o$) and uniform (n=o) field. Thus the linearized Hamiltonian for the corrections is:

$$\mathcal{H}_o = \frac{1}{2}\frac{p_x^2}{p_o} + \frac{1}{2}\frac{p_z^2}{p_o} - eB_c x \tag{2.4}$$

Let's now introduce in the Hamiltonians the so-called linear perturbations:
a) field errors, $\Delta B = B - B_o$
b) magnetic element misalignments, Δx and Δz
c) dipole tilts around the axis s, θ
d) stray magnetic field, ΔB

These errors cause linear about x and z members to appear in the Hamiltonians:

$$\mathcal{H} = \mathcal{H}_o + \delta\,\mathcal{H}^{(1)} \tag{2.5}$$

where:

$$\delta\,\mathcal{H}^{(1)} = \begin{cases} -e\Delta B_z x + \dfrac{p_o}{\rho}\,\theta z + \dfrac{p_o(1+n)}{\rho^2}x\Delta x - \dfrac{p_0 n}{\rho^2}z\Delta z + (1+\dfrac{x}{\rho})\Delta p\,, & \textit{for dipoles} \\ egx\Delta x - egz\Delta z\,, & \textit{for quadrupoles} \end{cases} \tag{2.6}$$

The quadratic part $\mathcal{H}_o$ of the Hamiltonian (2.5) describes particle oscillations, as long as the linear part $\delta\mathcal{H}^{(1)}$ causes an internal force depending on the variable s. This is the well-known classical mechanics case of forced small oscillations. Because of the internal force, the orbit is distorted. The new orbit is a periodical solution of the Hamilton equations:

$$\begin{aligned} \frac{dx_{co}}{ds} &= \frac{\partial\mathcal{H}}{\partial p_{x,co}} \\ \frac{dp_{x,co}}{ds} &= -\frac{\partial\mathcal{H}}{\partial x_{co}} \\ x_{co}(s+2\pi R) &= x_{co}(s) \\ p_{x,co}(s+2\pi R) &= p_{x,co}(s) \end{aligned} \tag{2.7}$$

In (2.7) R is the mean radius of the accelerator.

Equations equivalent to (2.7) are valid for the vertical plane as well.

Let u and p_u be the conjugate variables describing the oscillations around the orbit:

$$\begin{aligned} x &= x_{co} + u \\ p &= p_{x,co} + p_u \end{aligned} \tag{2.8}$$

If we now perform a canonical transformation from the variables x, p_x to u, p_u using as a generating function:

$$f_2(x,p_u,s) = (p_{x,co}(s) + p_u)x - x_{co}(s)p_u \tag{2.9}$$

We shall obtain for the new Hamiltonian:

$$\begin{aligned} K\,(u,p_u,v,p_v,s) &= \mathcal{H}(x_{co}(s)+u,\ p_{x,co}(s)+p_u,\ z_{co}(s)+v,\ p_{z,co}(s)+p_v,s) + \frac{\partial F_2}{\partial s} \\ &= \mathcal{H} - \left(\frac{\partial \mathcal{H}}{\partial x_{co}}\, u + \frac{\partial \mathcal{H}}{\partial p_{x,co}}\, p_u + \frac{\partial \mathcal{H}}{\partial z_{co}}\, v + \frac{\partial \mathcal{H}}{\partial p_{z,co}}\, p_v \right) \end{aligned} \tag{2.10}$$

The Hamiltonian K does not contain linear in u, p_u, v, p_v members i.e. it describes only the particle oscillations around the closed orbit.

From the Hamiltonians (2.3,2.6) one can deduce the equations of the transverse particle motion. In the Newton's form they are:

$$\begin{aligned} \frac{d^2x}{ds^2} + k_x(s)x &= F_x(s) \\ \frac{d^2z}{ds^2} + k_z(s)z &= F_z(s) \end{aligned} \tag{2.11}$$

where:

$$k_x(s) = \begin{cases} \dfrac{(1-n)}{\rho^2}, & \textit{for dipoles} \\ 0, & \textit{for correctors} \\ -\dfrac{g}{B_o\rho}, & \textit{for quadrupoles} \end{cases} \tag{2.12}$$

$$k_z(s) = \begin{cases} \dfrac{n}{\rho^2}, & \textit{for dipoles} \\ o, & \textit{for correctors} \\ \dfrac{g}{B_o\rho}, & \textit{for quadrupoles} \end{cases} \tag{2.13}$$

$$F_x(s) = \begin{cases} -\dfrac{\Delta B_z}{B_o\rho} - \dfrac{(1+n)}{\rho^2}\,\Delta x, & \textit{for dipoles} \\ -\dfrac{B_c}{B_o\rho}, & \textit{for correctors} \\ -\dfrac{g\Delta x}{B_o\rho}, & \textit{for quadrupoles} \end{cases} \tag{2.14}$$

$$F_z(s) = \begin{cases} -\dfrac{n}{\rho^2}\Delta z - \dfrac{\theta}{\rho}, & \textit{for dipoles} \\ -\dfrac{B_c}{B_o\rho}, & \textit{for correctors} \\ -\dfrac{g\Delta x}{B_o\rho}, & \textit{for quadrupoles} \end{cases} \tag{2.15}$$

3. Closed Orbit

The equations (2.11) are Hill's equations with a non-zero right hand side. Its general solution can be represented as a sum of the general solution of the homogeneous equation and a particular solution of the non-homogeneous one. The latter can be taken as periodic, keeping in mind the accelerator symmetry. This periodic particular solution will describe the closed orbit as long as the general solution of the homogeneous equation describes the particle oscillation.

The particle oscillations in an accelerator can be described by the Twiss's amplitude function $\beta(s)$[3] :

$$x(s) = a\sqrt{\beta(s)}\cos\left(Q\int_0^s \frac{ds}{Q\beta(s)}\right) \tag{3.1}$$

where Q is the number of the betatron oscillations per turn.

Let us introduce the new variables:

a) generalized azimuth:

$$\varphi = \int_0^s \frac{ds}{Q\,\beta(s)} \tag{3.2}$$

b) normalized deviation:

$$\eta = \frac{x}{\sqrt{\beta(s)}} \tag{3.3}$$

In these new variables the oscillations (3.1) can be written as:

$$\eta(\varphi) = a\cos(Q\varphi) \tag{3.4}$$

By implication we shall describe the closed orbit using the variables (3.2, 3.3).

Using the properties of the β function it is possible to transform the equation (2.11) to an equation of forced oscillations:

$$\frac{d^2\eta}{d\varphi^2} + Q^2\eta = Q^2 f(\varphi) \tag{3.5}$$

where:

$$f(\varphi) = \beta^{3/2}(\varphi)F(\varphi) \tag{3.6}$$

Using the method of varying the integration constants the following periodical particular solution of (3.5) can be obtained[4] :

$$\eta = \frac{Q}{2\sin\pi\, Q} \int_{\varphi}^{\varphi+2\pi} f(t)\cos Q(\varphi+\pi-t)\, dt \tag{3.7}$$

The integral representation (3.7) is the base formula for the closed orbit description. There exist two approaches to the closed orbit treatment:

a) A matrix approach.

As the perturbations are equal to zero out of the magnetic elements ($f(\varphi) = 0$) and the elements are short enough compared to the accelerator circumference ($\Delta\varphi << 2\pi$) the integral (3.7) can be transformed to the sum:

$$\eta(\varphi_i) = \frac{Q}{2\sin\pi Q} \sum_{\substack{j=1 \\ \varphi_i \le \varphi_j \le \varphi_i+2\pi}}^{M+L} \bar{f}_i\, \Delta\varphi_j \cos Q(\varphi_i+\pi-\varphi_j) \tag{3.8}$$

Here M is the total number of the dipoles, L the number of quadrupoles and the bar above a symbol means averaging over the magnetic element.

It is convenient to put (3.8) in the matrix form:

$$\eta_i = \sum_{\substack{j=i \\ \varphi_i \le \varphi_j \le \varphi_i+2\pi}}^{M+L} A_{ij}\, \delta_j \tag{3.9}$$

where:

$$A_{ij} = \cos Q(\varphi_i+\pi-\varphi_j) \tag{3.10}$$

and:

$$\delta_j = \begin{cases} -\dfrac{Q\overline{\beta_j^{3/2}}\Delta\varphi_j}{2\sin\pi Q}\Delta B_j - \dfrac{Q\overline{\beta_j^{3/2}}\eta_j\Delta\varphi_j}{2\sin\pi Q\rho_j^2}\Delta x_j\,, & \textit{for dipoles} \\ -\dfrac{Q\overline{\beta_j^{3/2}}\Delta\varphi_j}{2\sin\pi Q}B_{cj}\,, & \textit{for correctors} \\ -\dfrac{Q\overline{\beta_j^{3/2}}g_j\Delta\varphi_j}{2\sin\pi QB\rho}\Delta x_j\,, & \textit{for quadrupoles} \end{cases} \tag{3.11}$$

The reason for introducing the generalized perturbations δ_j is that they have the same dimensions as the normalized orbit η, i.e. $m^{1/2}$.

b) Harmonic analysis approach.

The orbit $\eta(\varphi)$ is periodic with a period of 2π. Let us expand it in a Fourier series:

$$\eta(\varphi) = \frac{u_o}{2} + \sum_{k=1}^{\infty} (u_k\cos k\varphi + v_k\sin k\varphi) \tag{3.12}$$

Let us also expand the perturbations $f(\varphi)$ in a Fourier series:

$$f(\varphi) = \frac{f_o}{2} + \sum_{k=1}^{\infty} (f_k\cos k\varphi + g_k\sin k\varphi) \tag{3.13}$$

From the equation (3.5) the following relation between the Fourier coefficients of the orbit and the perturbations can be deduced:

$$\begin{aligned} u_o &= f_o \\ u_k &= \left(\frac{Q^2}{Q^2-k^2}\right) f_k \\ v_k &= \left(\frac{Q^2}{Q^2-k^2}\right) g_k \end{aligned} \tag{3.14}$$

Of course the matrix and the harmonic orbit treatments give the same results which can be demonstrated using the formula:

$$\cos Q(\varphi_i + \pi - \varphi_j) = (\sin \pi Q)\ \frac{2Q}{\pi} \left(\frac{1}{2Q^2} - \sum_{k=1}^{\infty} \cos k \frac{(\varphi_i - \varphi_j)}{k^2 - Q^2} \right) \tag{3.15}$$

4. Error Sources

The linear perturbations causing the closed orbit distortion can be summarized in the following way.

a) constant errors

i) errors in the coercive force.

These kind of errors can be estimated approximately by:

$$\Delta B \approx - \mu_o \frac{\ell_{st}}{\ell_a} \Delta H_c \tag{4.1}$$

where ℓ_{st} is the magnet core length and ℓ_a is the aperture.

ii) errors due to eddy currents

iii) stray magnetic fields

iv) earth magnetic field

b) errors proportional to the main magnetic field

i) permeability errors. Approximately:

$$\frac{\Delta B}{B} \approx \left(\frac{\ell_{st}}{\mu_r^2 \ell_a}\right) \Delta \mu \tag{4.2}$$

ii) errors in the magnet core length

$$\frac{\Delta B}{B} \approx - \frac{1}{\mu_r \ell_a + \ell_{st}} \Delta \ell_{st} \tag{4.3}$$

iii) aperture errors

$$\frac{\Delta B}{B} \approx - \frac{1}{\frac{\ell_{st}}{\mu_r} + \ell_a} \Delta \ell_a \tag{4.4}$$

iv) adjustment errors — element misalignments, median plane displacements, dipole tilts, quadrupole magnetic center displacements, errors in the coil positions, etc.

v) ground movement

c) errors appearing only in high fields— these are errors due to saturation.

In the case of the COSY cooler synchrotron the first magnetic measurements show that random relative field errors with a standard deviation:

$$\sigma_{\Delta B/B} = 2.10^{-4} \tag{4.5}$$

can be expected.

According to the machine design the misalignment errors are going to be:

$$\begin{aligned} \sigma_{\Delta x} &= \sigma_{\Delta z} = \sigma_{\Delta s} = 0{,}25\ mm \\ \sigma_{\Theta} &= 0{,}3\ mrad \end{aligned} \tag{4.6}$$

5. COSY Orbit Simulation Tools. Interactive Computer Program ORBIT

Many of the widespread computer codes designed for accelerators development such as DIMAD, PETROS, MAD, etc., have features for closed orbit simulation and correction.

For the case of COSY orbit treatment we used the computer program MAD[5]: MAD possesses features for orbit simulation under the influence of misalignment and field errors, and it use the MICADO algorithm for orbit correction.

Besides MAD, we developed an interactive computer program called ORBIT, especially intended for closed orbit simulation and correction[6]. ORBIT is a Pascal program designed for IBM personal computers (200K—long source code). It has menu driven interface and enhanced graphical capabilities. The initial data about the accelerator—elements, β-functions, phases, lengths and strengths— can be given either by a user-written file or by the MAD output file *Twiss*. Given the random errors in field and position, ORBIT is able to simulate the closed orbit, the Fourier spectrum of the orbit, and to prepare a histogram of the maximum orbit deviations for 200 accelerators with different random error distributions. ORBIT can estimate analytically the standard deviation of the orbit and of the orbit maximum. Given the orbit displacements read by the beam position monitors (BPM), ORBIT is able to produce an orbit draft, to interpolate the orbit deviations between BPMs and to approximate the orbit spectrum. The interpolation is done using Lagrange and cubic spline methods— Appendix 2.

For the calculation of the Fourier spectrum of the orbit, Bessel coefficients, broken line and parabolic approximations are used— Appendix 3.

ORBIT includes six methods for orbit correction: Harmonic correction, beam-bump, LSQ method, Bacconier's method, DINAM and LSQ method with coupled correctors.

Fig. (1-8) show the results of COSY closed orbit simulation. We assumed error levels given in (4.5, 4.6).

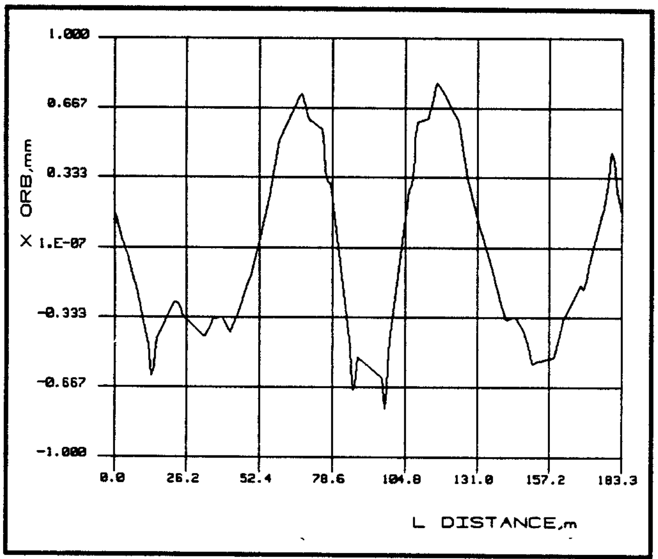

Figure 1 COSY horizontal closed orbit caused by a field error $\Delta B/B = 2 \cdot 10^{-4}$ in the first dipole.

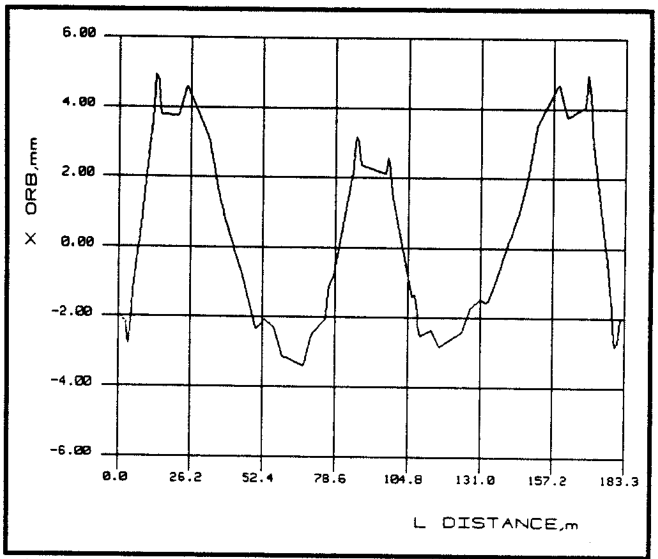

Figure 2 COSY horizontal closed orbit due to random field errors $\sigma_{\Delta B/B}=2 \cdot 10^{-4}$ in the dipoles.

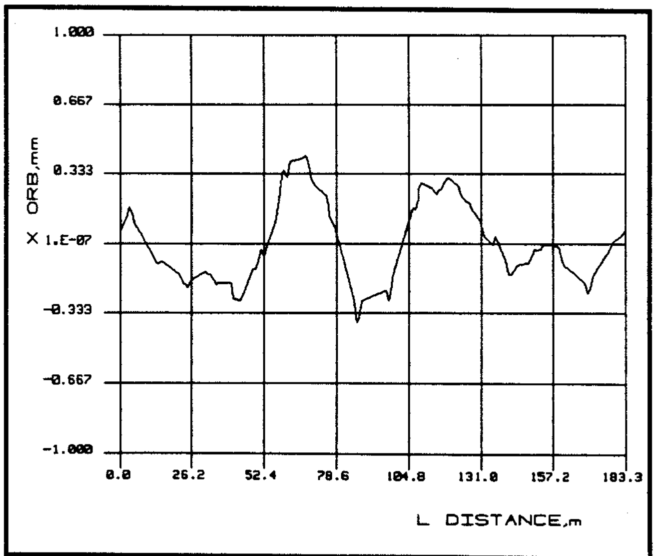

Figure 3 COSY horizontal closed orbit due to longitudinal displacements of the dipoles by $\sigma_{\Delta s}$ = 0.25 mm

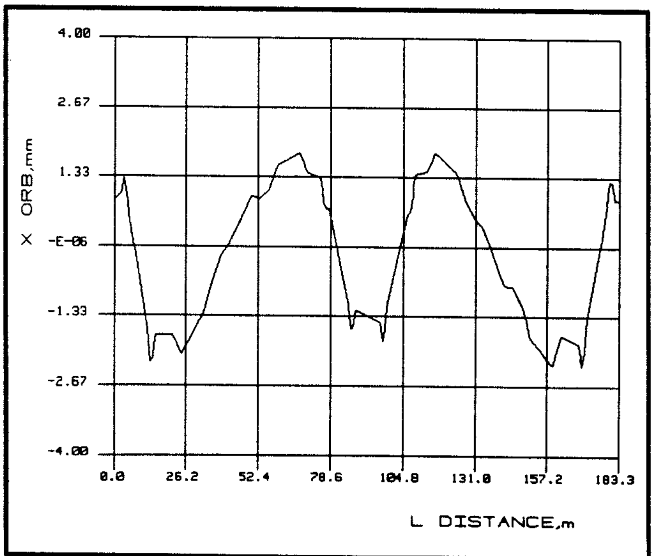

Figure 4 COSY horizontal closed orbit due to traversal displacements of the unit quadrupoles by $\sigma_{\Delta x}$ = 0.25 mm.

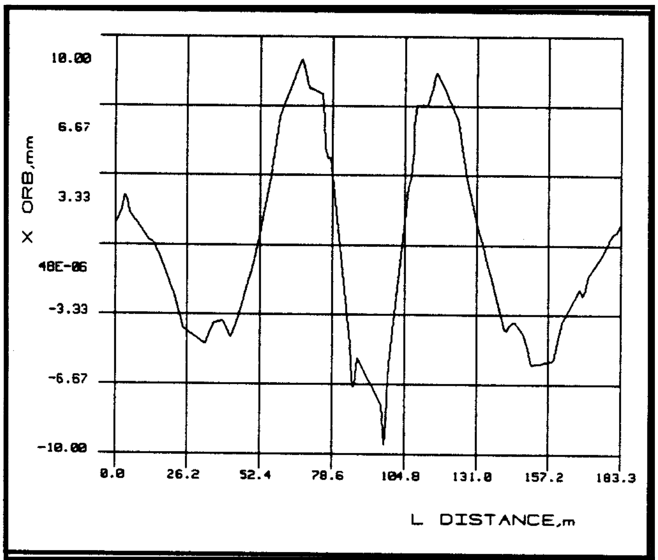

Figure 5 COSY horizontal closed orbit caused by a transversal displacement $\sigma_{\Delta x}$=0.25 mm of all quadrupoles.

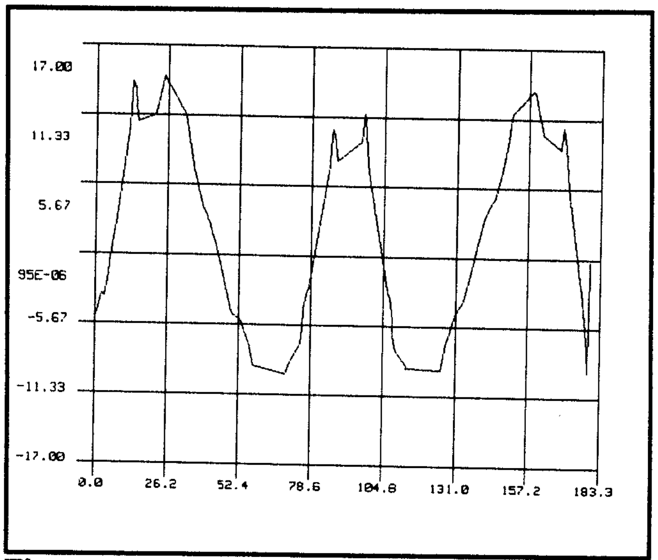

Figure 6 COSY horizontal closed orbit due to random field errors $\sigma_{\Delta B/B}=2\cdot10^{-4}$ in the dipoles and displacement $\sigma_{\Delta x}$=0.25 mm of all quadrupoles.

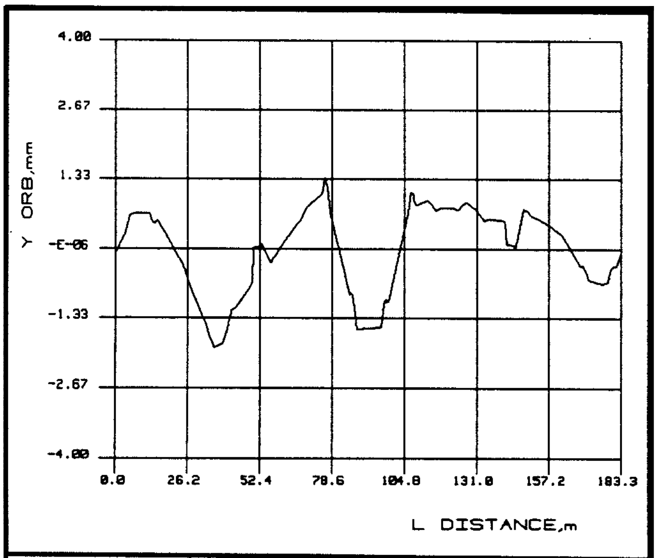

Figure 7 COSY vertical closed orbit due to tiltes of the dipoles around the longitudinal axe by $\sigma_{\Delta\theta}$ = 0.3 mrad.

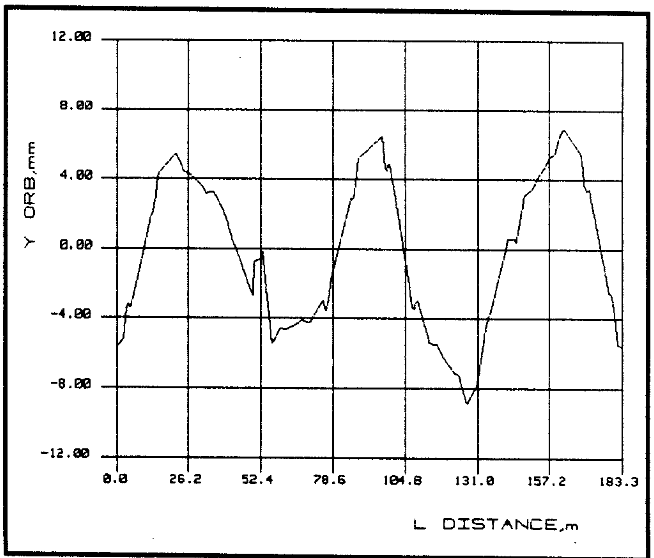

Figure 8 COSY vertical closed orbit due to displacements of the quadrupoles by $\sigma_{\Delta z}$ = 0.25 mm.

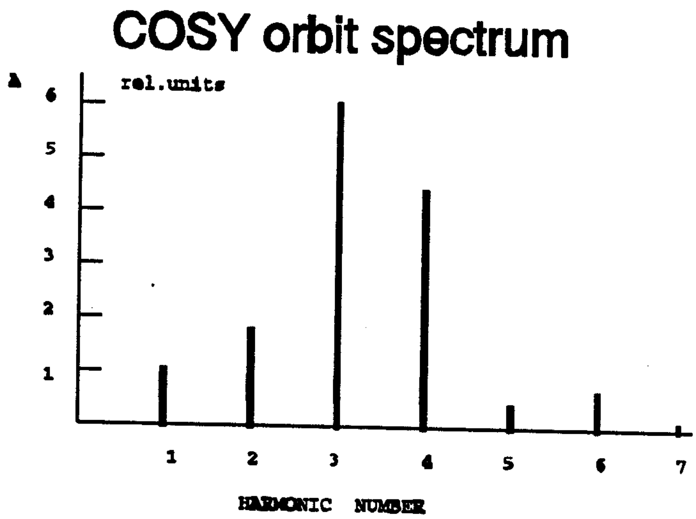

FIG.9. A case of COSY horizontal orbit Fourier spectrum. Q_x=Q_y= 3.38.

In these simulations and further in this paper the $Q_x = Q_z = 3.38$ COSY working point was examined. Fig. 9 shows a case of the COSY horizontal orbit Fourier spectrum.

6. Statistical Characteristics of the Perturbations and the Orbit

The perturbations ΔB and Δx are random functions of the generalized azimuth φ. Keeping in mind that they are non-zero only within the magnetic elements and that these elements are short enough compared to the accelerator circumference ($\Delta\varphi \ll 2\pi$) one can represent perturbations as sums of elementary random functions— $\Delta B_i \Pi_i(\varphi)$ and $\Delta x_i \Pi_i(\varphi)$, where ΔB_i and Δx_i are random values and $\Pi_i(\varphi)$ are single rectangular pulses of length $\Delta\varphi_i$. The random values ΔB_i
and Δx_i are uncorrelated, normally distributed, with a zero mathematical expectation and with standard deviations $\sigma_{\Delta B}$, $\sigma_{\Delta x}$ equal for all elements.

Let's expand the perturbations in a Fourier's series:

$$\Delta B(\varphi) = \frac{a_0}{2} + \sum_{k=1}^{\infty} (a_k \cos k\varphi + b_k \sin k\varphi) \tag{6.1}$$

The Fourier's amplitudes a_k and b_u are random values. Their mathematical means vanish and their variances are:

$$\begin{aligned} D(a_0) &= \sigma_{\Delta B}^2 \sum_{j=1}^{M} \left(\frac{\Delta\varphi_j}{2\pi}\right)^2 \\ D(a_k) &= \sigma_{\Delta B}^2 \sum_{J=1}^{M} \left(\frac{\cos k\varphi_j \Delta\varphi_j}{\pi}\right)^2 \\ D(b_k) &= \sigma_{\Delta B}^2 \sum_{j=1}^{M} \left(\frac{\sin k\varphi_j \Delta\varphi_j}{\pi}\right)^2 \end{aligned} \tag{6.2}$$

In uniform magnetic structures consisting of p equal periods the formulae (6.2) are simplified leading to a "white" spectrum:

$$D(a_k) = D(b_k) = \frac{1}{2} D(a_0) = \frac{\sigma_{\Delta B}^2 P}{2\pi^2} \sum_{j=1}^{M_p} \Delta\varphi_j^2 \tag{6.3}$$

In (6.3) M_p is the number of dipoles per period. Using the accelerator symmetry it is possible to demonstrate as well that $M(a_k b_k)=0$, i.e. that a_k and b_k are non-correlated. Analogical results can be obtained for Δx.

Let us now discuss the statistical characteristics of the orbit itself.

From (3.9) it follows that the orbit deviation η_i as a sum of normally distributed values is normally distributed itself, with an expected value of zero and a variance:

$$D(\eta_i) = \left(\frac{Q}{2B_0\rho\sin\pi Q}\right)^2 \left[\sigma_{\Delta B}^2 \sum_{j=1}^{M} \beta_j^3 \, \Delta\varphi_j^2 \cos^2 Q(\varphi_i+\pi-\varphi_j) + \sigma_{\Delta x}^2 \sum_{j=1}^{L} g_j^2 \, \beta_j^3 \, \Delta\varphi_j^2 \cos^2 Q(\varphi_i+\pi-\varphi_j)\right] \tag{6.4}$$

In uniform magnetic structures, (6.4) is simplified:

$$D(\eta_i) = \left(\frac{Q}{2B_0\rho\sin\pi Q}\right)^2 p\, \sigma_{\Delta B}^2 \sum_{j=1}^{M_p} \frac{\beta_j^3\, \Delta\varphi_j^2}{2} + \left(\frac{Q}{2B_0\rho\sin\pi Q}\right)^2 p\, \sigma_{\Delta x}^2 \sum_{j=1}^{L_p} \frac{g_j^2\, \beta_j^3\, \Delta\varphi_j^2}{2} \tag{6.5}$$

In the same way the statistical characteristics of the orbit divergence $\eta'(\varphi)$ can be calculated and one obtains that for uniform structures:

$$D(\eta') = Q^2\, D(\eta) \tag{6.6}$$

Successful accelerator operation requires that the maximum orbit deviation η_{max} and its statistical characteristics be known.

As for every accelerator from a large group of accelerators with different random error distributions, the maximum orbit deviation η_{max} appears at a different point φ_{max}. η_{max} is not normally distributed.

It is very difficult to obtain the statistical characteristics of η_{max} in the general case. As a rough approximation let us restrict ourselves to the major $k \approx Q$ harmonic in the orbit expansion (3.12):

$$\eta(\varphi) \approx u_k \cos k\varphi + v_k \sin k\varphi = A\cos(Q\varphi + \alpha_k) \tag{6.7}$$

It is easy to see that in this approximation M $(\eta, \eta') = 0$, i.e. $\eta$and η' are statistically independent.

We have for the two-dimensional probability[7]:

$$p\left(\eta, \frac{\eta'}{Q}\right) = \frac{1}{2\pi\, \sigma_\eta^2} \exp\left(-\frac{A^2}{2\sigma_\eta^2}\right) \tag{6.8}$$

Obviously the orbit amplitude probability p(A) can be obtained by integrating (6.8) along a circle with radius A in the plane $\left(\eta, \frac{\eta'}{Q}\right)$: :

$$p\,(A) = \int_0^{2\pi} p\left(\eta, \frac{\eta'}{Q}\right) A\, d\varphi = \frac{A}{\sigma_\eta^2} \exp\left(-\frac{A^2}{2\sigma_\eta}\right) \tag{6.9}$$

Formula (6.9) represents Rayleigh's probability distribution:

$$p(A) = \frac{2A}{\sigma_A^2} \exp\left(-\frac{A^2}{\sigma_A^2}\right) \tag{6.10}$$

with—

$$\sigma_A = \sqrt{2}\sigma_\eta = \sqrt{2}\ \sigma_{u_k} = \sqrt{2}\ \sigma_{v_k} \tag{6.11}$$

The integral distribution function for the Rayleigh distribution is:

$$\phi\ (A) = 1 - \exp\left(-\frac{A^2}{\sigma_A^2}\right) \tag{6.12}$$

A better estimate will be achieved if two contributing harmonics $k < Q < (k+1)$ are taken into account. In this approximation:

$$\eta(\varphi) \approx u_k \cos k\varphi + v_k \sin k\varphi + u_{k+1} \cos(k+1)\varphi + v_{(k+1)} \sin(k+1)\varphi = \quad (6.13)$$
$$(u_k + u_{k+1} \cos\varphi + v_{k+1} \sin\varphi) \cos k\varphi \; + \; (v_k - u_{k+1} \sin\varphi + v_{k+1} \cos\varphi) \sin k\varphi$$

i.e., we have a harmonic oscillation with a slowly changing amplitude $A(\varphi)$:

$$A^2(\varphi) = (u_k + u_{k+1} \cos\varphi + v_{k+1} \sin\varphi)^2 + (v_k - u_{k+1} \sin\varphi + v_{k+1} \cos\varphi)^2 \qquad (6.14)$$

From (6.14) the maximum amplitude can be calculated:

$$A = \max A(\varphi) = r_k + r_{k+1} \qquad (6.15)$$

where:

$$r_k^2 = u_k^2 + v_k^2; \quad r_{k+1}^2 = u_{k+1}^2 + v_{k+1}^2 \qquad (6.16)$$

As it has already been demonstrated above, r_k and r_{k+1} which are the random amplitudes of the k^{th} and $(u+1)_{th}$ harmonics have Rayleigh's distributions. These amplitudes are statistically independent. From these assumptions the following expression for the variance of the maximum amplitude can be derived[8]

$$\sigma_A^2 = R_k^2 + \frac{\pi}{2} R_k R_{k+1} + R_{k+1}^2 \qquad (6.17)$$

where:

$$R_k^2 = 2\sigma_{u_k}^2; \quad R_{k+1}^2 = 2\sigma_{u_{k+1}}^2 \qquad (6.18)$$

In[8] it has been also shown that the probability for the orbit amplitude to be greater than A is:

$$F(A) = 2\sqrt{\pi}\frac{R_k R_{k+1}}{R_k^2 - R_{k+1}^2} \frac{A}{\sqrt{R_k^2 + R_{k+1}^2}} \exp\left(-\frac{A}{R_k^2 + R_{k+1}^2}\right) \qquad (6.19)$$

In[8] it has been shown that the best agreement between the analytical estimates and the results of the computer simulation of the closed orbit can be achieved if the major three or four harmonics of the perturbations are taken into account. As the exact solution in this approximation is accompanied by great mathematical difficulties only an approximate estimation for the orbit amplitude variance is carried out:

$$\frac{\sigma_A^2}{\sum R_j^2} = \left(1 + \frac{\pi}{2} \frac{\sum\limits_{i,j}^{i \neq j} R_i R_j}{\sum R_j^2}\right) \tag{6.20}$$

$$F(A) = (4\pi)^{\frac{m-1}{2}} \prod_{j=1}^{m} \left(\frac{R_j}{\sqrt{\sum R_j^2}}\right) \exp\left(-\frac{A^2}{\sum R_j^2}\right) \sum_{i=0}^{\frac{m-1}{2}} \frac{(-1)^i \, (m-1)!}{2^{2i} \, i! \, (m-1-2i)!} \times \left(\frac{A}{\sqrt{\sum R_j^2}}\right) \tag{6.21}$$

where m is the number of used harmonics.

Using the above formulae COSY orbit probabilities have been evaluated. With the error levels (4.5, 4.6) we achieved the following data.

1. Horizontal Plane

A. For the Orbit

a) with dipole field errors $\sigma\Delta B/B = 2.10^{-4}$:

$$\sigma_x = 1.70\ mm; \quad \max\ \sigma_x = 2.69\ mm$$
$$(in\ the\ place\ where\ \beta = \max)$$

b) with one quadrupole displacement of $\sigma_{\Delta x} = 0.25$ mm:

$$\sigma_x = 1.00\ mm; \quad \max\ \sigma_x = 1.05\ mm$$

c) with all quadrupoles displaced with $\sigma_{\Delta x}$= 0.25 mm:

$$\sigma_x = 3.23\ mm; \quad \max\ \sigma_x = 4.71\ mm$$

d) with dipole field errors of $\sigma_{\Delta B/B}$= 2.10^{-4} and all quadrupoles displaced with $\sigma_{\Delta x}$= 0.25 mm:

$$\sigma_x = 3.65\ mm; \quad \max\ \sigma_x = 5.43\ mm$$

B. For the Orbit Amplitude

a) with dipole field errors of $\sigma_{\Delta B/B}$= 2.10^{-4}:

$$\sigma_A = 3.27 mm; \quad p(A > 6.55 mm) = 0.018$$

b) with one quadrupole displaced by $\sigma_{\Delta x}$= 0.25 mm:

$$\sigma_A = 1.76 mm; \quad p(A > 3.51 mm) = 0.007$$

c) with all quadrupoles displaced with $\sigma_{\Delta x}$= 0.25 mm:

$$\sigma_A = 6.89 mm; \quad p(A > 3.71 mm) = 0.005$$

d) with dipole field errors of $\sigma_{\Delta B/B}$= 2.10^{-4} and all quadrupoles displaced with $\sigma_{\Delta x}$= 0.25 mm:

$$\sigma_A = 7.64 mm; \quad p(A > 15.30 mm) = 0.005$$

2. Vertical Plane

A. For the Orbit

a) with dipole tilts of σ_Θ= 0.3 mrad:

$$\sigma_z = 1.42\ mm; \quad \max\ \sigma_z = 2.09 mm$$

b) with random displacements of all quadrupoles with $\sigma_{\Delta z}$= 0.25 mm:

$$\sigma_z = 2.32 mm; \quad \max\ \sigma_z = 2.92 mm$$

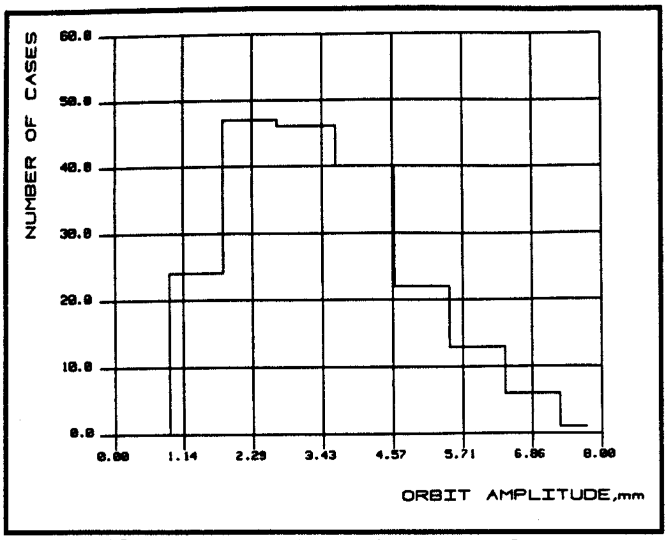

Figure 10. Horizontal plane.Histogram of the maximum orbitdeviations for 200 machines with random dipole field errors $\sigma_{\Delta B/B}=2.10^{-4}$.

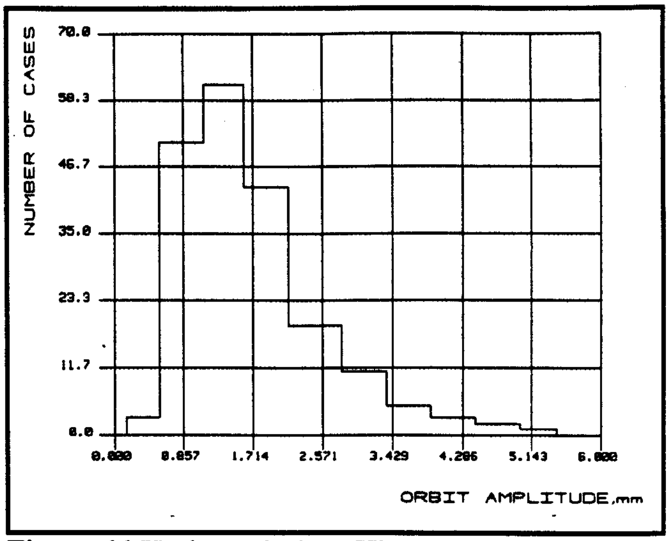

Figure 11. Horizontal plane.Histogram of the maximum orbit deviations for 200 machines with random displacements $\sigma_{\Delta x}$=0.25 mm of the unit quadrupoles.

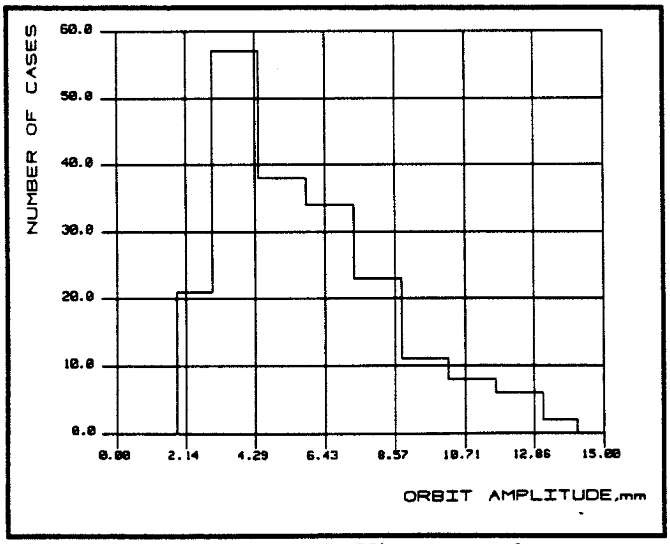

Figure 12. Horizontal plane.Histogram of the maximum orbit deviations for 200 machines with random displacements $\sigma_{\Delta x}$=0.25mm of all quadrupoles.

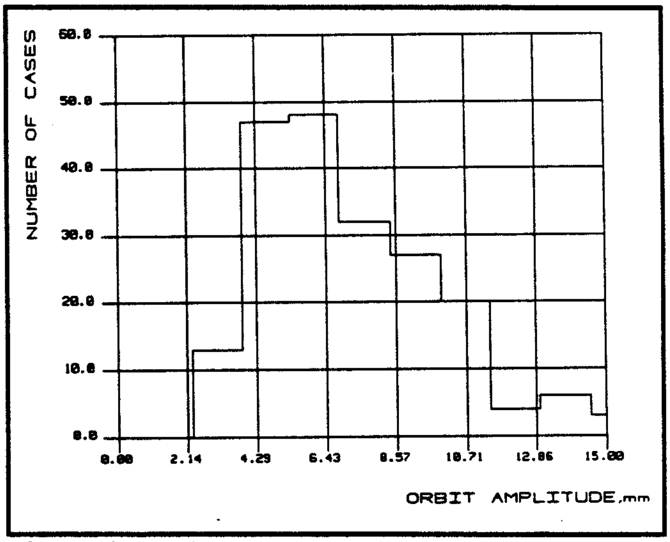

Figure 13. Horizontal plane.Histogram of the maximum orbit deviations for 200 machines with random field errors $\sigma_{\Delta B/B}=2.10^{-4}$and quads displ.$\sigma_{\Delta x}$=0.25mm.

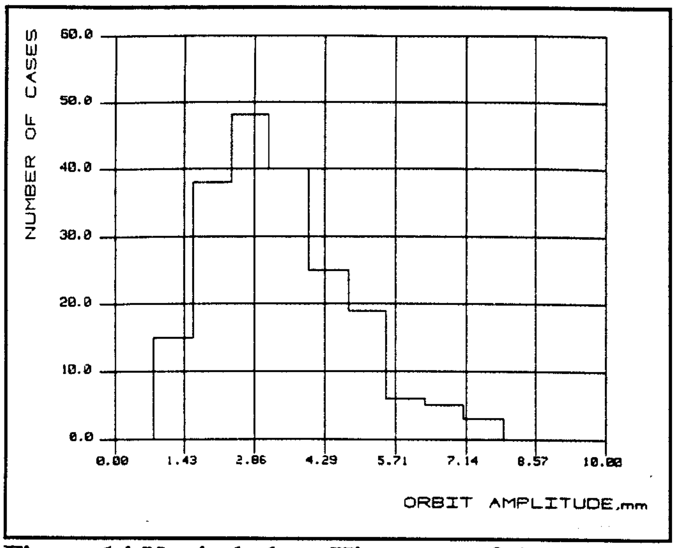

Figure 14. Vertical plane. Histogram of the maximum orbit deviations for 200 machines with random dipole tilts σ_θ=0.3 mrad.

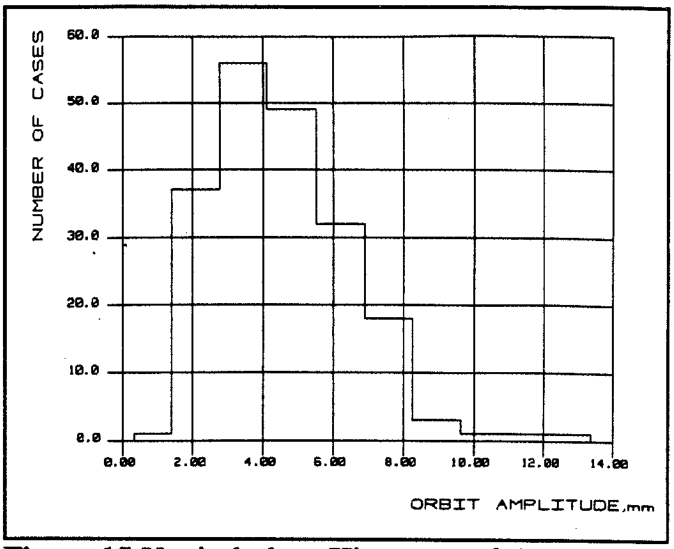

Figure 15. Vertical plane. Histogram of the maximum orbit deviations for 200 machines with random displacements of all quadrupoles with $\sigma_{\Delta z}$=0.25mm.

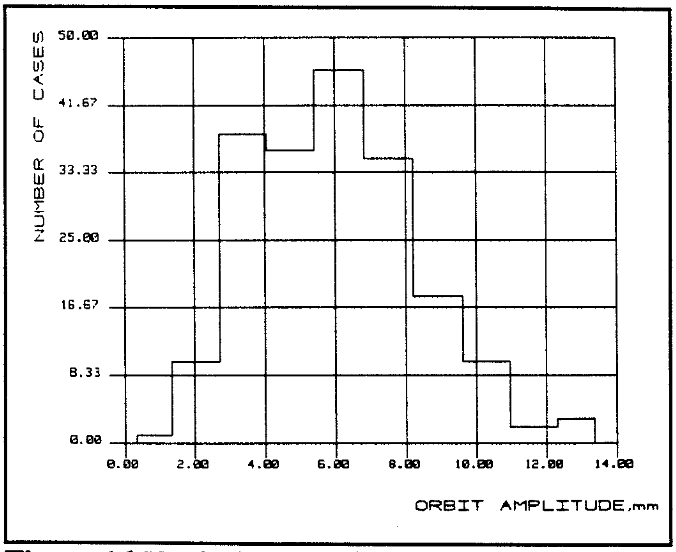

Figure 16. Vertical plane. Histogram of the maximum orbit deviations for 200 machines with random dipole tilts σ_θ=0.3mrad and displacements of all quadrupoles $\sigma_{\Delta z}$=0.25mm.

c) with dipole tilts of σ_Θ= 0.3 mrad and random displacements of all quadrupoles with $\sigma_{\Delta z}$= 0.25 mm:

$$\sigma_z - 2.73 mm; \quad \max \sigma_z - 3.59 \; mm$$

B. For the Orbit Maximum

a) with dipole tilts of σ_Θ= 0.3 mrad:

$$\sigma_A - 2.19 \; mm; \quad p(A > 4.38 mm) - 0.005$$

b) with random displacements of all quadrupoles with $\sigma_{\Delta z}$= 0.25 mm:

$$\sigma_A - 5.16 mm; \quad p(A > 10.31 mm) - 0.005$$

c) with dipole tilts of σ_Θ= 0.3 mrad and displacements of all quadrupoles with $\sigma_{\Delta z}$=5.60 mm:

$$\sigma_A - 5.60 mm; \quad p(A > 11.2 mm) - 0.005$$

Using the computer programs ORBIT and MAD, we simulated the maximum orbit deviation for the case of the COSY cooler synchrotron. Figures (10-16) show the results for 200 machines with different distributions of the random errors.

7. A General Description of the Orbit Correction Methods

In accelerators as a rule the number of beam position monitors (N) is less than the numbers of dipoles (M) and quadrupoles (L)— $N < M+L$. This means that from the readings of the BPMs we can calculate only a part of the perturbations—correction with uncertainty.

The general block diagram of the orbit correction is shown of Fig. 17. Fig.18 gives a classification of the orbit correction methods.

The orbit correction methods can be divided into two main groups— methods for local correction and methods for correction of the orbit over the whole ring (general correction).

The local correction methods correct the orbit only in a part of the accelerator circumference. Outside of this region, the orbit is unchanged.

The methods for general correction cover methods that try to compensate perturbations directly and methods in which a kind of goal function, depending on the orbit deviations and corrector strengths, is minimalized.

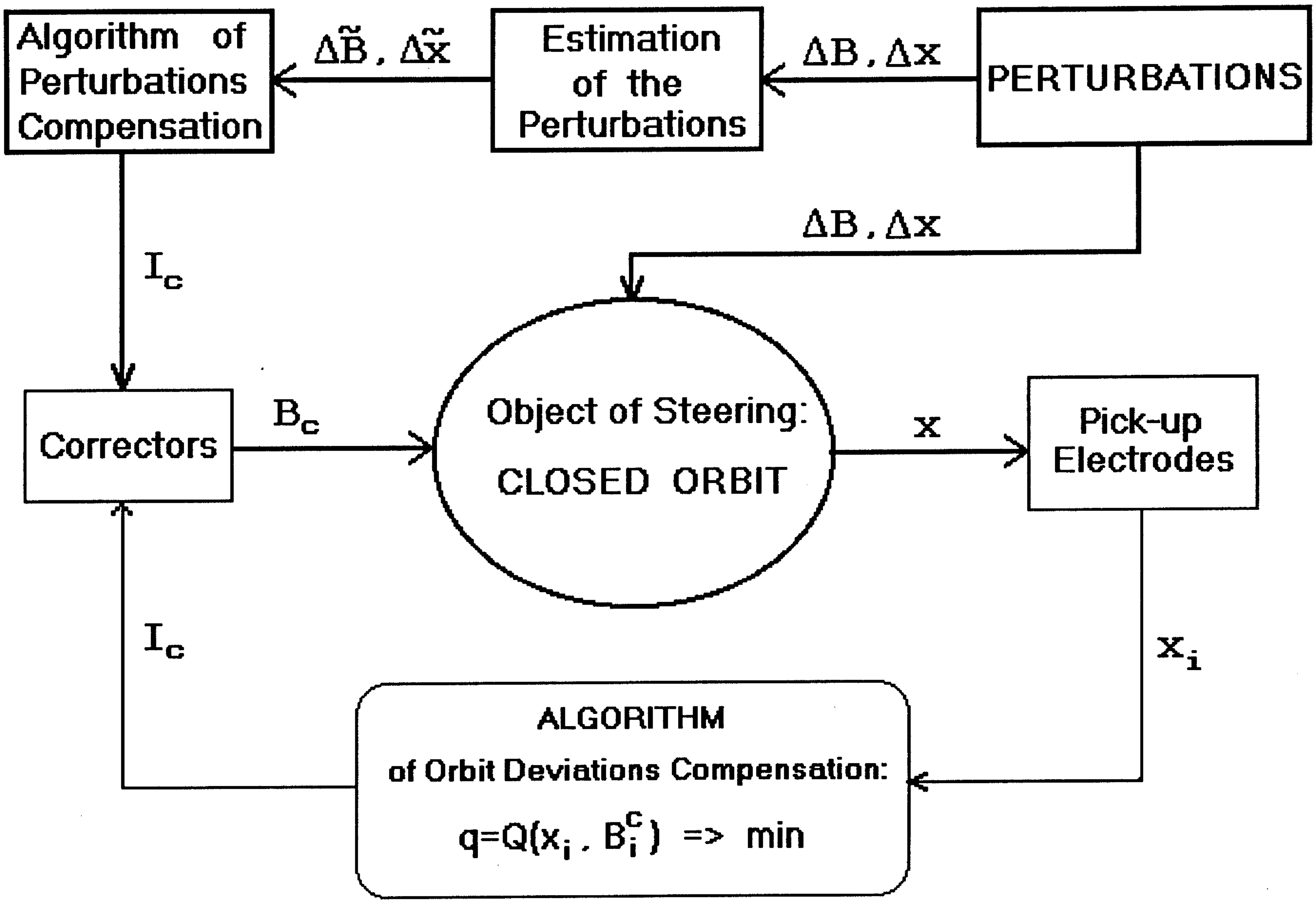

Fig. 17. Block diagram of orbit correction

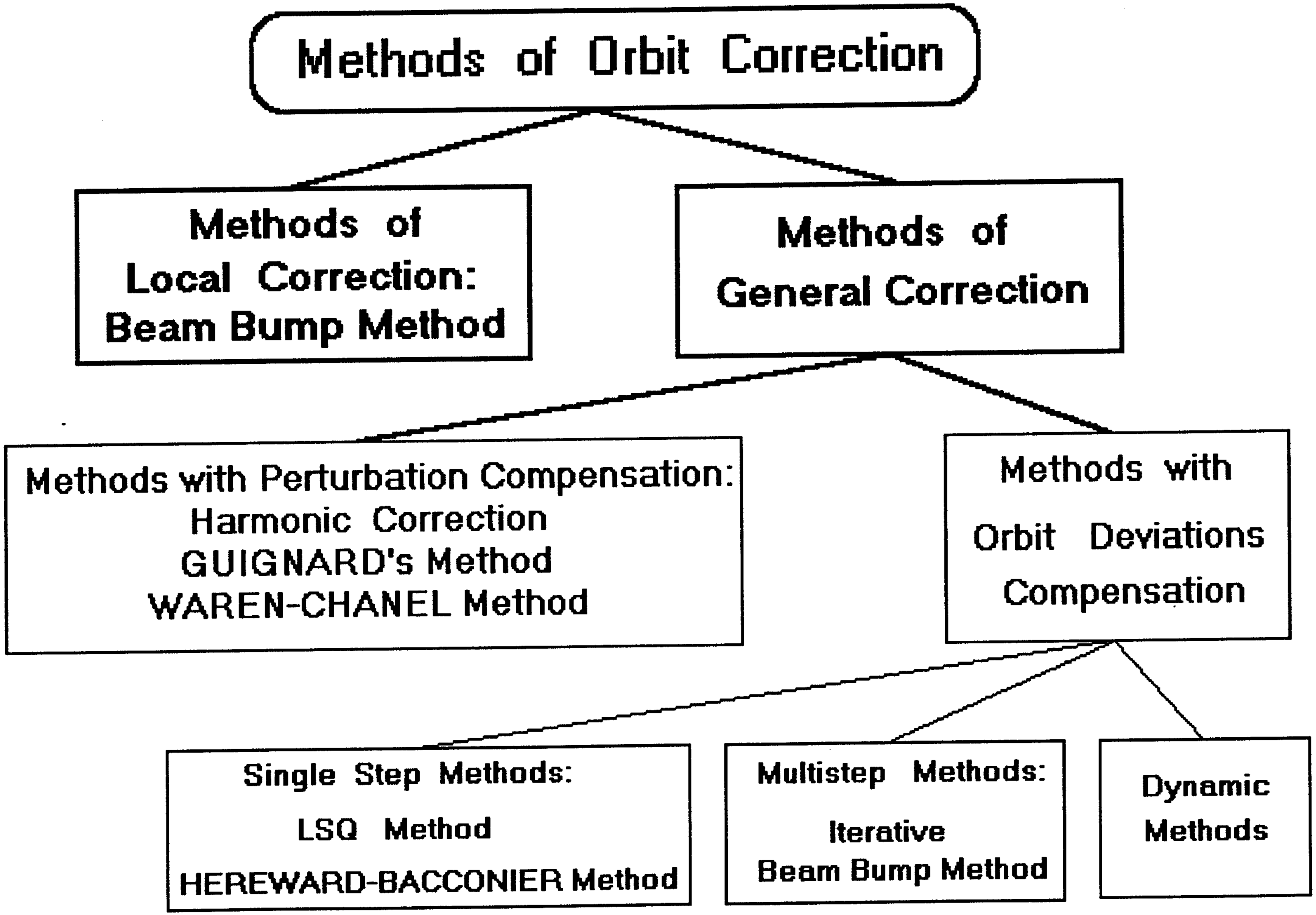

Fig. 18. Classification of orbit correction methods

The methods with perturbation compensation try to assess the perturbation strengths.

In the harmonic correction, this is achieved through the approximate values of the first perturbation harmonics. In the method proposed by G. Guignard and its later improvements, the "probability" of having errors in a given area of the accelerator circumference is found. Finally, in the Warren and Channell's suggestion, the values of all the errors are calculated, applying a special measurement procedure.

After the perturbations have been assessed, corrections with proper values and positions are applied in order to compensate the orbit deviations.

In the methods with orbit deviation compensation a quality criterion is created. It can be either a function or a functional, from the orbit deviations and correctors strengths. Then the minimum of the quality criterion is chosen. The single-step, the multi-step, and the dynamical methods are included in this group.

In the single-step method, the orbit is considered only at the points where BPMs are situated and is characterized by the state vector $\vec{x} = (x_1, x_2, \ldots, x_n), x_i$ being orbit deviations. A goal function:

$$q = Q(\vec{x}, \vec{B}_c) \tag{7.1}$$

is created.

In (7.1), $\vec{B}_c$ is a vector whose components are correctors strengths. They are determined so that q has a minimum.

In the multi-step methods, the whole accelerator circumference is divided into separate areas. At first, the orbit over the first area is corrected. After that we go to the next area taking into consideration the results from the correction in the former step and so on.

The dynamical methods of correction treat the orbit as a whole curve $\eta(\varphi)$ rather than just orbit deviations in BPMs $\eta_i = \eta(\varphi_i)$. The quality criterion is a functional:

$$I = \int_0^{2\pi} Q(\eta(\varphi), B_c(\varphi))\, d\varphi \tag{7.2}$$

The condition for I to have a minimum gives us the chosen corrector strengths.

We fulfilled a computer simulation of COSY orbit correction applying many of the methods mentioned above.

COSY orbit control system will use 27 capacitive pick-up monitors for each plane—Table 1. Eight correcting dipoles in the straight sections and back leg correcting windings in all bending dipoles are available for horizontal orbit correction. In the computer simulation, we have used only back-leg windings for the horizontal orbit correction in the banding magnets with numbers: 1, 4, 6, 8, 9, 12, 13, 16, 20, 22, 24.

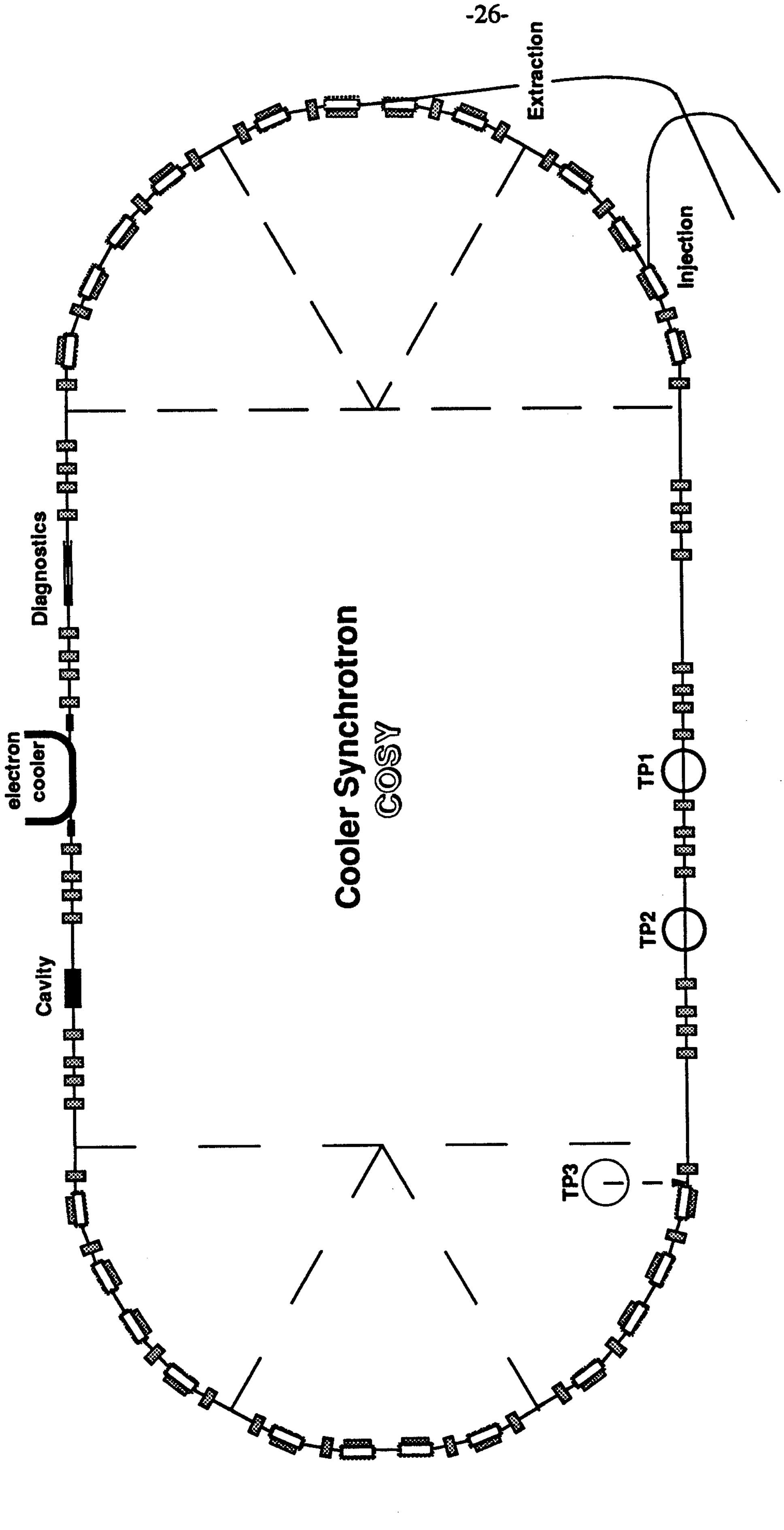
Extraction
Injection
Diagnostics
electron
cooler
Cavity
Cooler Synchrotron
COSY
TP1
TP2
TP3

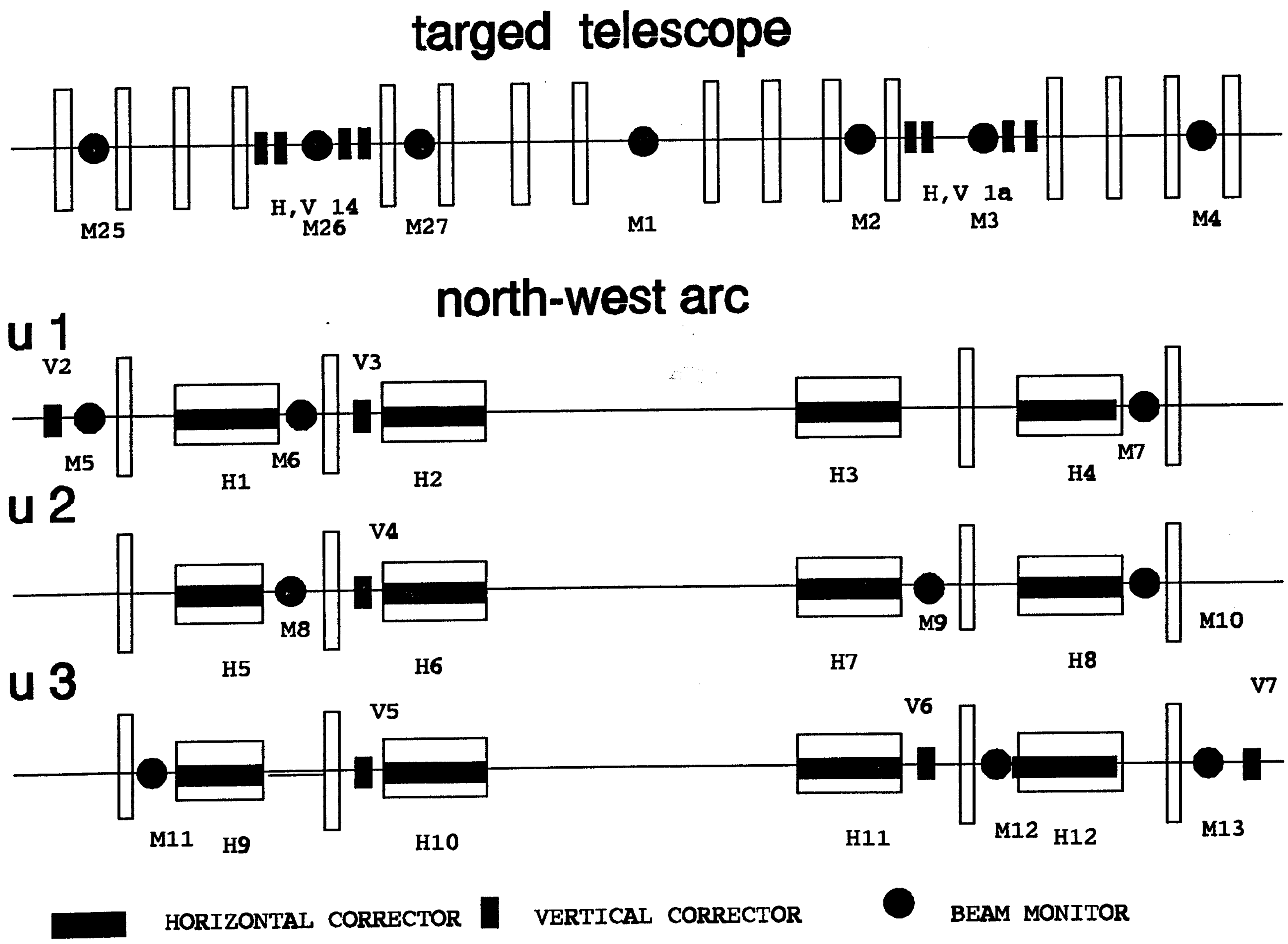
targed telescope
M25
H,V 14
M26
M27
M1
M2
H,V 1a
M3
M4
north-west arc
u 1
V2
M5
H1
M6
V3
H2
H3
H4
M7
u 2
H5
M8
V4
H6
H7
M9
H8
M10
u 3
M11
H9
V5
H10
H11
V6
M12
H12
V7
M13
HORIZONTAL CORRECTOR
VERTICAL CORRECTOR
BEAM MONITOR

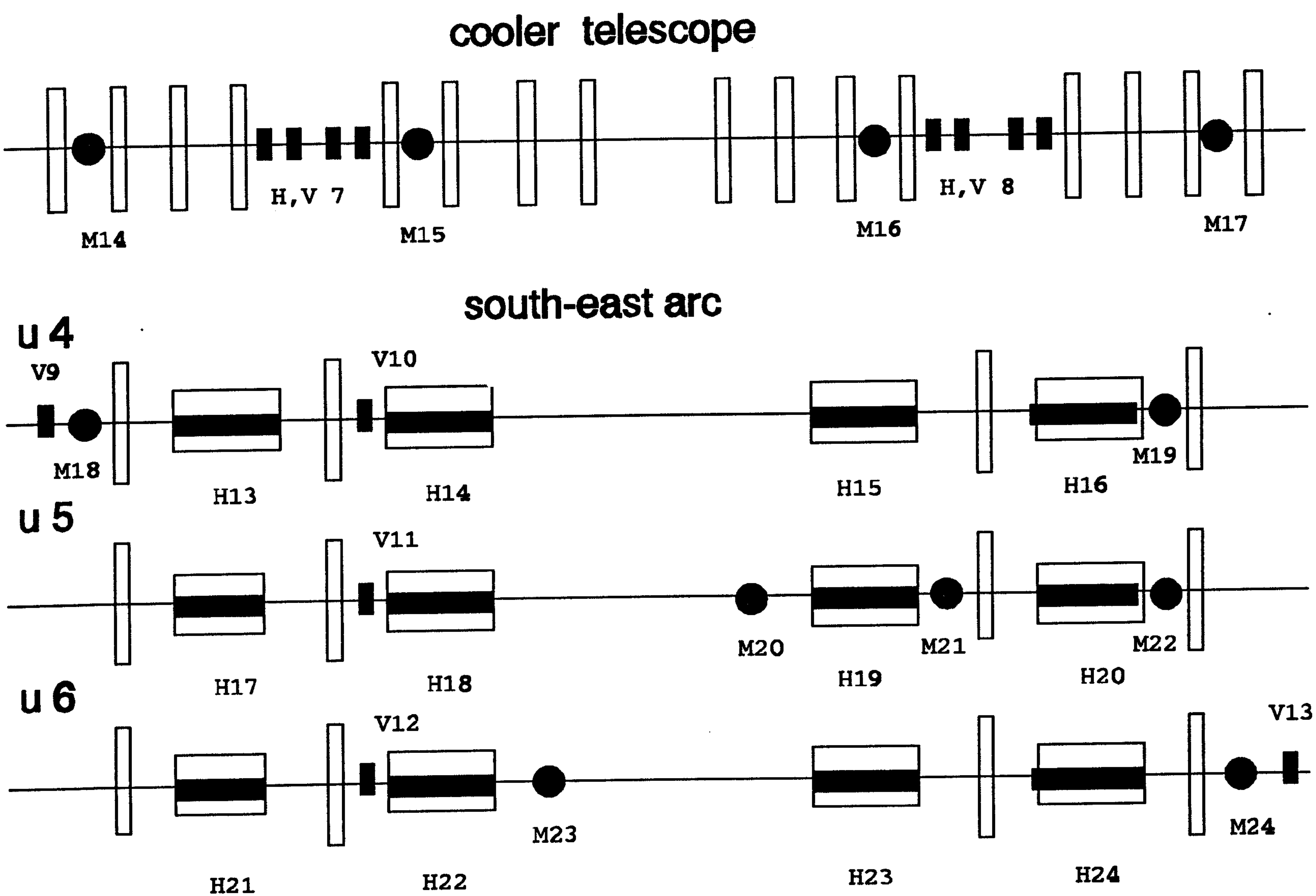

TABLE 1.COSY BEAM POSITION MONITORS AND CORRECTORS

Seventeen vertical steering magnets will be installed for the vertical orbit correction, 11 of them in the bending sections and 8 in the straight sections.

8.Correction Methods with Compensation of the Perturbations

8.1 Harmonic Correction Method

In the harmonic correction method, the orbit Fourier spectrum:

$$\eta(\varphi) = \frac{u_0}{2} + \sum_{k=1}^{\infty} (u_k \cos k\varphi + v_k \sin k\varphi) \qquad (8.1.1)$$

is calculated at first.

As we know, the orbit deviations only in the points where BPMs are situated and not the whole curve $\eta(\varphi)$ the methods of the applied harmonic analysis have to be used— Appendix 3. According to Appendix 3, measuring the orbit with 2N BPMs we can determine only the approximate values of the first N orbit Fourier harmonies. The simplest way is to approximate first orbit harmonics with the so-called Bessee's coefficients:

$$\begin{aligned} u_0 &\approx U_0 = \frac{1}{N}\sum_{i=1}^{2N} \eta_i \\ u_k &\approx U_k = \frac{1}{N}\sum_{i=1}^{2N} \eta_i \cos k\varphi_i, \quad (k=1,2,...,N) \\ v_k &\approx V_k = \frac{1}{N}\sum_{i=1}^{2N} \eta_i \sin k\varphi_i, \quad (k=1,2,...,(N-1)) \end{aligned} \qquad (8.1.2)$$

In Appendix 3 some better approximations are also given.

Knowing the orbit harmonics, the perturbation harmonics can be calculated using (3.14).

In the harmonic correction method, the fields in 2N correcting dipoles are chosen so that the first N perturbations harmonies to be canceled[9-11].

Keeping in mind that the correcting dipoles are short $(\Delta\varphi_c < 2\pi)$ and transforming integrals to sums, we are to solve therefore the following system of equations:

$$\frac{1}{\pi}\sum_{i=1}^{2N} f_i^c \, \Delta \varphi_i^c = U_0$$
$$\frac{1}{\pi}\sum_{i=1}^{2N} f_i^c \cos k\varphi_i \Delta \varphi_i = \frac{Q^2-k^2}{Q^2} U_k \qquad (8.1.3)$$
$$\frac{1}{\pi}\sum_{i=1}^{2N} f_i^c \sin k\varphi_i \Delta \varphi_i = \frac{Q^2-k^2}{Q^2} V_k$$

Then the fields in the correcting dipoles $B_i^c,\ i=1,2,\ldots,2N$ can be calculated from the generalized perturbations f_i^c using (3.6, 2.14, 2.15).

In the simplest case of correctors situated at equal distances along the accelerator circumference, the above system has a solution:

$$f_i^c \Delta \varphi_i = \frac{\pi}{N} U_0 + \qquad (8.1.4)$$
$$\frac{\pi}{N}\sum_{i=1}^{N-1} \frac{Q^2-p^2}{Q^2}\,(U_p \cos p\varphi_i + V_p \sin p\varphi_i) + \frac{\pi}{N}\left(\frac{Q^2-N^2}{Q^2}\right) U_N \cos N\varphi_i$$

In the general case of non-uniformly situated correctors, the system of equations (8.1.3) can be written in the matrix form:

$$C\vec{\delta} = \vec{x} \qquad (8.1.5)$$

where:

$$C_{ij} = \begin{cases} a, & i=1 \\ a\left(\dfrac{Q^2}{Q^2-k^2}\right)\cos k\varphi_j, & k=i-1;\ \ i=2,3,\ldots,(n+1) \\ a\left(\dfrac{Q^2}{Q^2-k^2}\right)\sin k\varphi_j, & k=i-(N+1);\ \ i= N+2,N+3,\ldots,2N \end{cases} \qquad (8.1.6)$$

$$a = \frac{2\sin\pi Q}{\pi Q} \tag{8.1.7}$$

and:

$$\vec{\delta} = (\delta_1, \delta_2, \ldots, \delta_{2N}) \tag{8.1.8}$$

is the vector of generalized perturbations (3.11)

$$\vec{x} = (\xi_0 u_0, \xi_1 u_1, \ldots, \xi_n u_n, \xi_1 v_1, \ldots, \xi_{n-1} v_{N-1}) \tag{8.1.9}$$

is the vector of the weighted orbit harmonics. In (8.1.9)ξ_i being either 0 or 1 are masks pointing out whether the corresponding harmonic has to be taken into account or not. The introduction of the masks (weights) ξ_i improves the method's reliability due to the removing of these harmonics which values are not reliably estimated.

Fig 19-20 show the results of the simulation of the harmonic correction of the COSY horizontal orbit. In Fig. 21, a histogram of the maximum deviations of the horizontal COSY orbit after a harmonic correction is given. This histogram covers 200 machines with different distributions of the random errors.

8.2 G. Guignard's Method

It is very important for the biggest error sources to be found. Then we can check more carefully the corresponding elements and the practice shows that in many cases after removing this very rough imperfection the maximum orbit deviation is reduced to sufficiently small values. As in an error-free area of the accelerator circumference, the RHS of equation (3.5) is equal to zero. The orbit in this error-free area is:

$$\eta = A\cos Q\varphi + B\sin Q\varphi + C \tag{8.2.1}$$

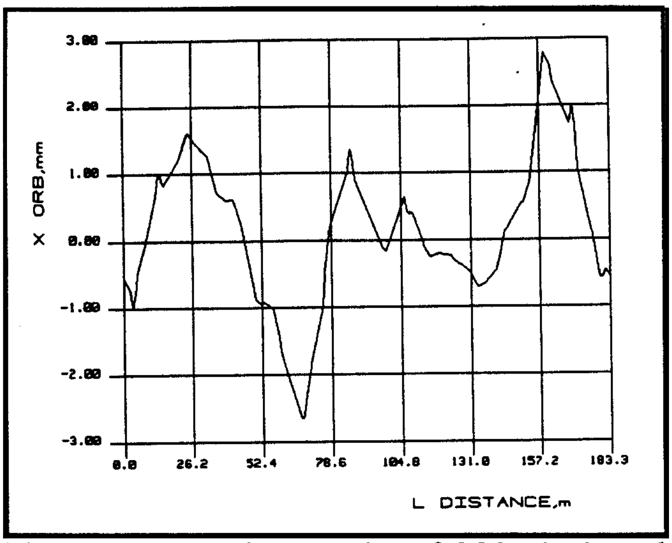

Figure 19. Harmonic correction of COSY horizontal orbit.1-4 harmonics corrected.

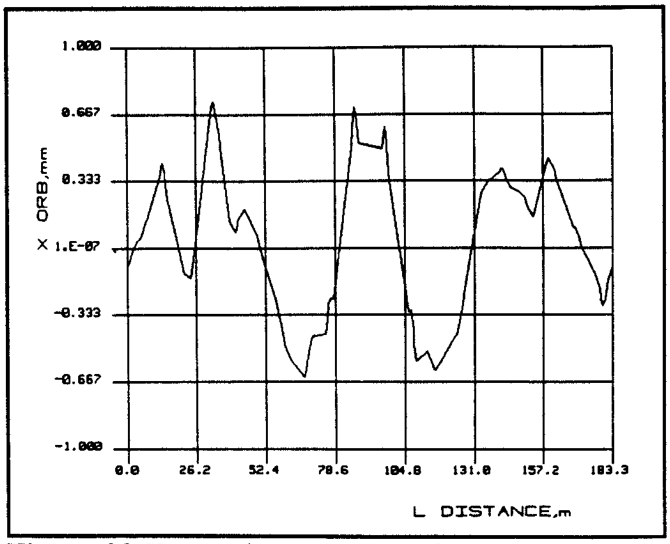

Figure 20. Harmonic correction of COSY horizontal orbit.1-10 harmonics corrected.

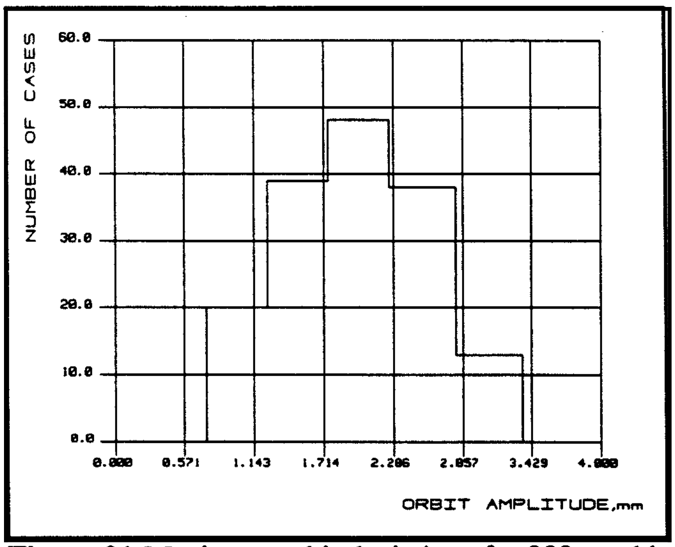

Figure 21. Maximum orbit deviations for 200 machines with different distributions of the errors after harmonic correction.

The orbit (8.2.1) should be matched to the whole orbit in both ends of the area under consideration. From here the constants A, B, C are calculated.

If now we assume that there are errors in the above area then the smooth solution (8.2.1) will not be valid any more. In the points with errors, η' will undergo kicks.

Obviously the divergence of the real measured orbit from the smooth model (8.2.1) will be a measure for the perturbation strengths in the area.

According to G. Guignard[12] we shall define the "probability" for the existence of perturbations in an area of the accelerator as:

$$\Psi = \frac{1}{n} \sum_{k=p}^{p+n-1} \left[\sqrt{\beta_k}(A\cos Q\varphi_k + B\sin Q\varphi_k + c) - x_k\right]^2 \tag{8.2.2}$$

In (8.2.2), p is the number of the first BPM and $n \geq 4$ is the whole number of BPMs included in the area.

The constant A, B, C in (8.2.2) defines the non-perturbated orbit. We shall determine their values so that the non-perturbated orbit will lie as close as possible to the readings x_k in the BPMs (in LSQ sense). In other words we calculate A, B, C from the condition $\Psi \rightarrow \min$.

In Guignard's method, we calculate the "probability" Ψ for successive areas of the accelerator ring. The areas with big Ψ values are possible sources of errors.

The G. Guignard's suggestion was improved later in CERN[13,14]
A kind of expert system based on formula (8.2.2) and including a lot of heuristic rules have been built.

8.3 Warren and Channell's Suggestion

In accelerators, as a rule, the number of BPMs— N is less than the numbers of dipoles—M and quadrupoles—L, $N<M+L$. Therefore we are not able to solve the system of equations (3.9) with respect to the errors. In[15] Warren and Channell suggest enlarging this system adding some new equations. For this purpose, new measurements of the orbit have to be done changing synchrotron parameters and keeping the errors unchanged. A new set of orbit measurement can be carried out changing the quadrupoles strengths (i.e. changing Q) or changing the signs of the quadrupole gradients (for example reducing FODO structure into DOFO). The enlarged system of equations is solved by the LSQ method.

9. Local Correction Methods.

9.1 Beam-Bump Method

At some places (injection, extraction, and others) a very high degree of orbit correction is necessary. From the other hand at some places of the accelerator ring the orbit deviation may be much greater than the average one due to strong local stray fields, strong local imperfections or ground movement. These require the development of methods for local correction.

Such local correction method is the beam-bump method, suggested by Collins in the sixties[16-20]

The idea of the beam-bump method consists in a local orbit correction by the means of three correcting dipoles—Fig. 22. The orbit deviation is compensated in a BPM situated near the middle corrector as long as out of the area occupied by the correctors the orbit is kept unchanged. Therefore we have the conditions:

$$
\begin{gathered}
x(\varphi_{PUE}) = -x_m \\
x(\varphi<\varphi_1,\varphi>\varphi_3) \equiv x'(\varphi<\varphi_1,\varphi>\varphi_3) \equiv 0
\end{gathered}
\tag{9.1.1}
$$

From (9.1.1) and (3.9) the following system of three equations about corrector strengths can be deduced:

$$
\begin{gathered}
\sin\mu_{12}\sqrt{\beta_2}\,\epsilon_2 + \sin\mu_{13}\sqrt{\beta_3}\,\epsilon_3 = 0 \\
\sqrt{\beta_1}\,\epsilon_1 + \cos\mu_{12}\sqrt{\beta_2}\,\epsilon_2 + \cos\mu_{13}\sqrt{\beta_3}\,\epsilon_3 = 0 \\
(ctg\ \pi Q\cos\mu_{1pue} + \sin\mu_{1pue})\sqrt{\beta_1}\,\epsilon_1 + \\
(ctg\ \pi Q\cos\mu_{pue2} + \sin\mu_{pue2})\sqrt{\beta_2}\,\epsilon_2 + \\
((ctg\ \pi Q\cos(\mu_{pue2}+\mu_{23}) + \sin(\mu_{pue2}+\mu_{23}))\sqrt{\beta_3}\,\epsilon_3 = \frac{2x_m}{\sqrt{\beta_{pue}}}
\end{gathered}
\tag{9.1.2}
$$

where:

$$
\epsilon = \frac{B_c \Delta s}{B\rho}
\tag{9.1.3}
$$

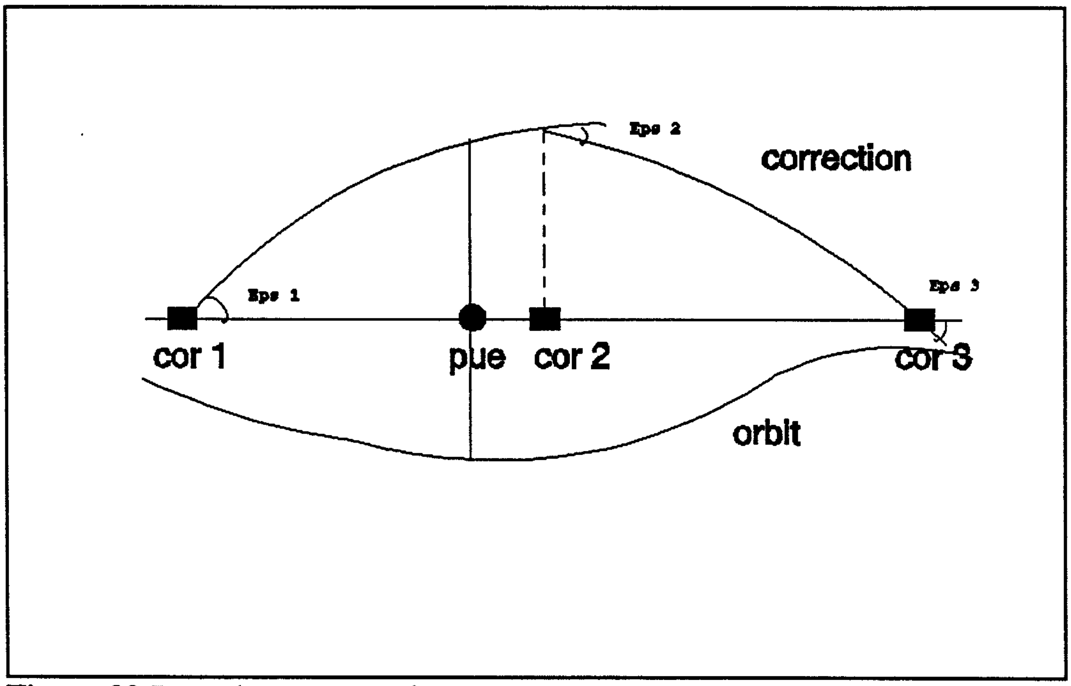

Figure 22. Beam-bump correction.

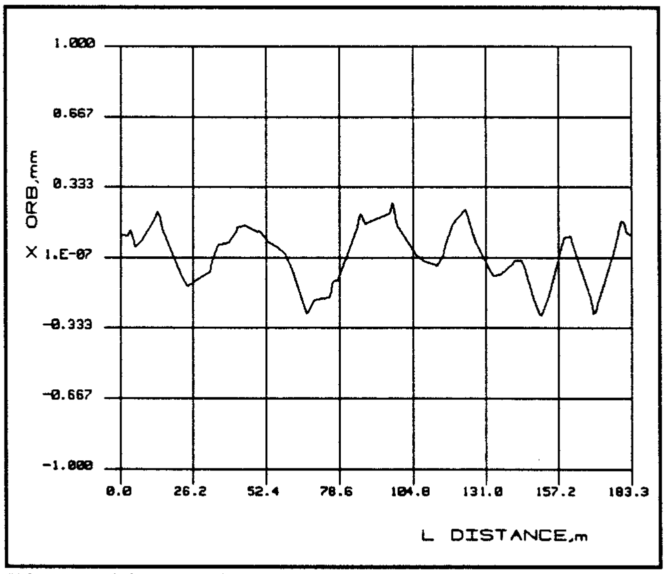

Figure 23. Iterative Beam-bump correction
of COSY horizontal orbit.

is the bump (kick) in the correcting dipole,

$$\mu_{12} = \int_{s1}^{s2} \frac{ds}{\beta(s)} = Q(\varphi_2 - \varphi_1) \tag{9.1.4}$$

is the betatron phase advance.

For the special case of a BPM situated very close to the central corrector, i.e. when $\mu_{pue2} \approx 0$ the system (9.1.2) is reduced to:

$$\begin{aligned} \epsilon_1 &= -\frac{\eta_m}{\sqrt{\beta_1}\sin\mu_{12}} \\ \epsilon_2 &= \frac{\sin(\mu_{12}+\mu_{23})}{\sin\mu_{12}\sin\mu_{23}} \frac{\eta_m}{\sqrt{\beta_2}\sin\pi Q} \\ \epsilon_3 &= -\frac{\eta_m}{\sqrt{\beta_3}\sin\mu_{23}} \end{aligned} \tag{9.1.5}$$

In the completely symmetrical case— $\mu_{12} = \mu_{23} = \mu, \quad \mu_{pue} = 0$:

$$\begin{aligned} \sqrt{\beta_1}\,\epsilon_1 &= \sqrt{\beta_2}\,\epsilon_2 = \frac{x_m}{\sqrt{\beta_{pue}}\sin\mu} \\ \sqrt{\beta_2}\,\epsilon_2 &= -\frac{2x_m}{\sqrt{\beta_{pue}}}\, ctg\ \mu \end{aligned} \tag{9.1.6}$$

Besides using the expression (3.9) about the closed orbit, we can obtain the system (9.1.2) in another way— by using the beam transport matrix between two arbitrary points s_1 and s_2 in Twiss' form:

$$M_{12} = \begin{bmatrix} \sqrt{\frac{\beta_2}{\beta_1}}(\cos\mu_{12} + \alpha_1\sin\mu_{12}) & \sqrt{\beta_1\beta_2}\sin\mu_{12} \\ \frac{1}{\sqrt{\beta_1\beta_2}}(-\sin\mu_{12} - \alpha_1\alpha_2\sin\mu_{12} + (\alpha_1-\alpha_2)\cos\mu_{12}) & \sqrt{\frac{\beta_1}{\beta_2}}\ (\cos\mu_{12} - \alpha_2\sin\mu_{12}) \end{bmatrix}$$

Let M^1 be the transport matrix from CD_1 to PUE; M^2— from CD_1 to CD_2 and M^3— from CD_2 to CD_3. Then from (9.1.1) it follows that:

$$
\begin{aligned}
\epsilon_1 &= \frac{x_m}{m^1_{12}} \\
\epsilon_2 &= -\frac{m^3_{11} m^2_{12}}{m^3_{12}}\epsilon_1 - m^2_{22}\epsilon_1 \\
\epsilon_3 &= -m^2_{12} m^3_{21}\epsilon_1 - m^3_{22}(m^3_{22}\epsilon_1^2 + \epsilon_2)
\end{aligned}
\tag{9.1.8}
$$

The optimum phase distance between the correctors in the tripole is $\mu \approx \frac{\pi}{2}$ when $\epsilon_2 \approx 0$

9.2 Generalizations of the Beam-Bump Correction Method

As a rule, the magnetic structure of storage rings and colliders is irregular. However, if the phase distance between BPM and CD_2 is big— fig.23, the beam-bump method correcting the orbit in the monitor closely to zero will increase the orbit deviation in CD_2. This happens when correctors and monitors are situated non-regularly (because of the lack of place) or when the betatron phase changes quite quickly (in the areas with small β). That is why some improvements of the beam-bump method have been put forward. Another reason for such improvements is the fact that in the beam-bump method $\epsilon_2 \sim 1/\sin\mu$ and in the case when $\mu \approx k\cdot\pi;\ k=1,2,...$ quite large corrector kicks will be necessary for a full correction to be fulfilled.

In[21] , groups of N monitors and K=N+2 correctors are used. The BPMs are considered to be situated close to the corresponding internal correctors.

The kicks of the internal correctors are determined by:

$$R\,\vec{\epsilon}_{int} = -\vec{x}_{pue} \quad (9.2.1)$$

where the matrix R is:

$$R_{ij} = \frac{\sqrt{\beta_i\beta_j}\sin_{jk}\sin\mu_{1i}}{\sin\mu_{1k}} \tag{9.2.2}$$

In (9.2.2), μ_{1i} is the phase advance between the first corrector and i-th internal corrector; μ_{jk} is the phase advance between the j-th internal corrector and the last corrector; μ_{1k} is the phase advance for the whole group correctors.

(9.2.1) is a generalization of (9.1.2) for the case of (N+2) correctors and N BPMs.

The two end kicks are determined in a way to keep the orbit out of the group unchanged.

$$\sqrt{\beta_1}\epsilon_1 = \frac{x_{pue1}}{\sqrt{\beta_{pue1}}\sin\mu_{1pue1}} \tag{9.2.3}$$

$$\sqrt{\beta_k}\epsilon_k = \frac{x_{pueN}}{\sqrt{\beta_{pueN}}\sin\mu_{pueNk}} \tag{9.2.4}$$

In the computer program PETROC (an improved CERN variant of the HERA's PETROS) another beam-bump improvement is done.[22,23] One can use K correctors, k being 0, 3, 4, 5. Between the correctors N≤2k beam position monitors are situated. No more that two BPMs can be placed between two correctors. Only three correctors are active (with non-zero kicks)— the first, the second, and the last. Let ϵ be the kick in the first active corrector.

In order for the orbit not to be changed, the two other active kicks have to be ϵr_2 and ϵr_k where:

$$r_2 = -\sqrt{\frac{\beta_1}{\beta_2}\frac{\sin\mu_{1k}}{\sin\mu_{2k}}} \tag{9.2.5}$$

$$r_K = \sqrt{\frac{\beta_1}{\beta_k}\frac{\sin\mu_{12}}{\sin\mu_{2k}}} \tag{9.2.6}$$

The kick ϵ in the first corrector is determined by the minimum of the function:

$$q = \sum_{BPMs} (x_i + x_{puei})^2 + w^2 \beta_1 \beta_2 \sin^2 \mu_{12} \epsilon^2 \tag{9.2.7}$$

In (9.2.7) x_{puei} is the measured orbit deviation and x_i is the orbit deviations due to correctors; w is a weight. The second member in (9.2.7) limits the corrector strengths.

10. Methods with Orbit Deviations Compensations

10.1 Iterative Beam-Bump Method

If we move consequently along the accelerator circumference, the local beam-bump method can be used as a method for general correction. Let the i-th step correctors with numbers (i-1)-th monitor. Therefore, each corrector works once as a first corrector in the correctors triple—fig.22, once as a second and once as a third corrector.

In this straightforward improvement, a little problem is hidden. In the beam-bump method, the correctors of the triple are tuned to cancel the orbit in the monitor which is situated as a rule near the middle corrector. Correctors affect the orbit locally; i.e. the impact of the correctors is equal to zero out of the triple. But as we pointed out above, in the iterative beam-bump the successive triples overlap a little (they have two common correctors). Hence, each corrector triple will cause a small orbit distortion in the next (belonging to the next triple) beam position monitor. The last correctors triple consisting of correctors (k-1), k and 1 will reduce the orbit deviation in the k-th monitor to zero, but will distort the orbit a little in the first monitor.

To avoid this trouble, one more turn of successive beam-bump corrections along the accelerator will be necessary. Fig. 23 shows the results of the simulation of the iterative beam-bump correction of the COSY horizontal orbit.

10.2 Least Squares Method

The method can be characterized as a single-step correction method.

The orbit is considered only in the points where beam position monitors are situated and is characterized by the state vector $\vec{\eta}^{\,c}$ corresponding to the corrections:

$$\vec{\eta} = \vec{\eta}^{(B+g)} + \vec{\eta}^{\,c} = \vec{\eta}^{(B+g)} + A\vec{\delta}^{\,c} \tag{10.2.1}$$

To write (10.2.1) we have used the formula (3.9), δ^c being the generalized corrections (3.11) and the fact that $\vec{\eta}^{B+g}$ are known from the BPMs readings.

In the least squares method (LSQ) the following goal function is minimized[11,24-26]

$$q = \sum_{i=1}^{N} \eta_i^2 = \vec{\eta}^{\,T}\vec{\eta} \to \min \tag{10.2.2}$$

It is important to not that as a rule the number of correctors—k is less than that of detectors—n i.e. K<N. It is possible to be demonstrated that the minimum of (10.2.2) occurs when corrector strengths are:

$$\vec{\delta}^{\,c}_{opt} = -(A^T A)^{-1} A^T \vec{\eta}^{(B+g)} \tag{10.2.3}$$

The minimum value of q (the so-called residual sum of squares) is equal to:

$$q_{\min} = \vec{\eta}^{(B+g)T}\vec{\eta}^{(B+g)T} A \vec{\delta}^{\,c}_{opt} \tag{10.2.4}$$

Fig. 24 shows the results of the LSQ correction of the COSY horizontal orbit.

10.3 Fast Realization of the LSQ Correction

A fast realization of the LSQ correction method is proposed in h.[21] The idea is at each iteration to optimize the orbit using only one corrector. Having tried in this way all available correctors, we choose for further use this one for which the residual sum of squares of orbit deviations is the smallest.

At the O-th iteration we begin with the orbit measured by BPMs:

$$\vec{\eta}^{(0)} = \vec{\eta}^{(B+g)} \tag{10.3.1}$$

Let $\vec{\eta}^{(n-1)}$ be the orbit having been optimized at the (n-1)-th iteration. As at each step at the n-th iteration, we will use only single correctors. Therefore:

$$\vec{\eta}_j^{(n)} = \vec{\eta}^{(n-1)} + \delta_j^{(n)} \vec{a}_j \tag{10.3.2}$$

where $\delta_j^{(n)}$ is the generalized strength of the j-th corrector at n-th iteration; $\vec{a}_j$ is the j-th column of the matrix (3.10).

Following the LSQ algorithm we will minimize:

$$q_j^{(n)} = \min_{\delta_j^{(n)}} (\vec{\eta}_j^{nT} \vec{\eta}_j^{(n)}) \tag{10.3.3}$$

Thus at the n-th iteration, we will obtain k values $q_j^{(n)}$, $j=1,2,\ldots,k$, one for each corrector. From these values $q_j^{(n)}$ we will choose the smallest one. The corresponding corrector will be the optimum corrector at the n-th iteration.Its optimum strength $\delta_{j(n)}$will be the correction used at the n-th iteration. Therefore our goal function is:

$$q_j^{(n)} \to \min_j \tag{10.3.4}$$

In [21], it is proved that this iterative procedure is convergent and that the corrector strengths found at different steps are added.

10.4 Algorithm MICADO

The MICADO algorithm for closed orbit correction was put forward by B Autin and Y. Marti in[27] and is realized in many accelerator design programs, for example in MAD[5]. This algorithm can be seen as an improvement of the LSQ method.

MICADO is an iterative algorithm. At the first iteration only single correctors are used. The goal function is as in the LSQ method:

$$q_j^{(1)} = \min_{\delta j} (\vec{\eta}_j^{(1)T} \vec{\eta}_j^{(1)}) \tag{10.4.1}$$

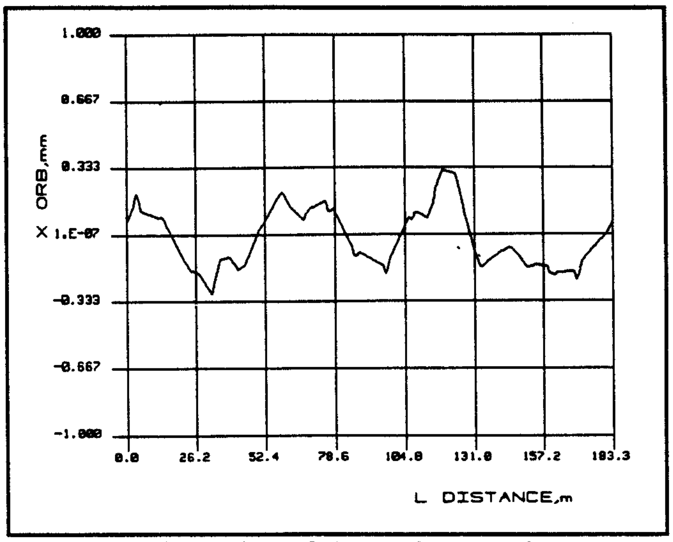

Figure 24. Simulation of the LSQ correction for COSY horizontal orbit.

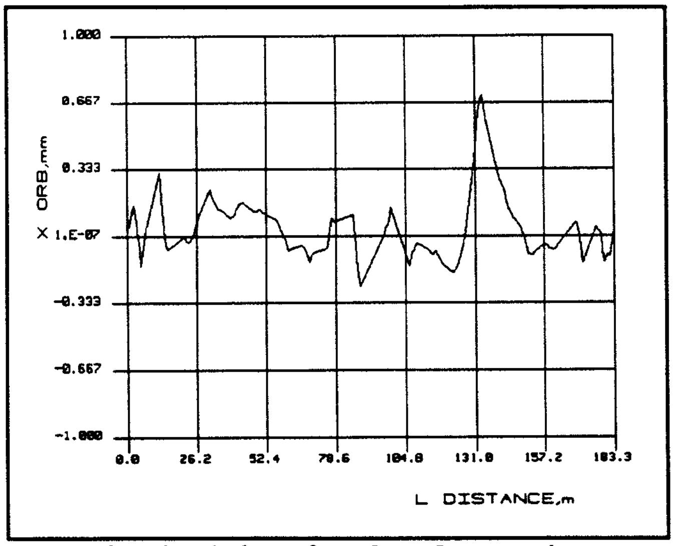

Figure 25. Simulation of MICADO correction for COSY horizontal orbit.

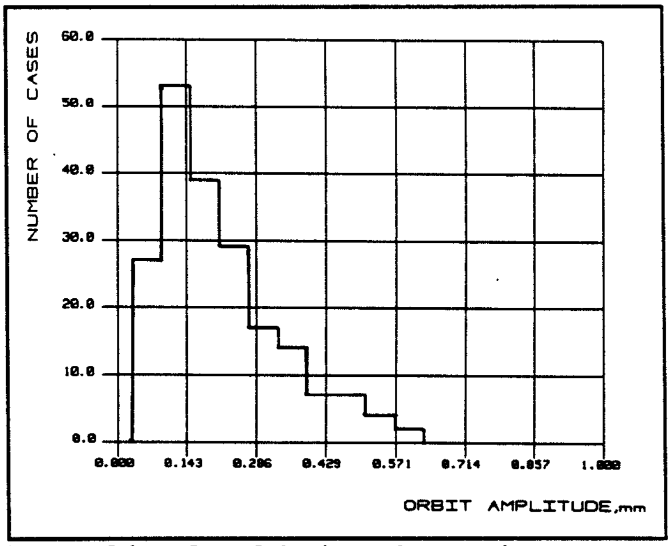

Figure 26.MICADO horizontal correction for 200 random machines.

where:

$$\vec{\eta}_j^{(1)} = \vec{\eta}^{(B+g)} + a\vec{\delta}_j^{(1)} \tag{10.4.2}$$

$\vec{\eta}^{(B+g)}$ being the vector of BPM readings and $\vec{\delta}_j^{(1)}$ being the vector of the generalized corrections (3.11). As at the first iteration we use only single correctors:

$$\vec{\delta}_j^{(1)} = (0,...,\delta_j^{(1)},...,0) \tag{10.4.3}$$

Therefore, at the first iteration we have to solve k equations with one unknown value— $\delta_j^{(1)},(j=1,2,...,k)$.

Next we find out the number j^* of that corrector among all k correctors for which $q_j^{(1)}$ (10.4.1) has the smallest value— $q_{j*}^{(1)}$.

It is j^*-th corrector that will be used at the second iteration together with each one of the rest (k-1) correctors. We minimize again the square function:

$$q_j^{(2)} = \min_{\delta j}(\vec{\eta}_j^{(2)T}\vec{\eta}_j^{(2)}) \tag{10.4.4}$$

But now the corrections vector $\vec{\delta}_j^{(2)}$ is:

$$\vec{\delta}_j^{(2)} = (0,...,\delta_{j*},...\delta j,...0) \tag{10.4.5}$$

i.e. has two non-zero components— one δ_{j*} the strength of the j*-th corrector (remember that this number was found and fixed at the previous step) and another one— the strength of any other corrector. Thus at the second iteration we have to solve (k-1) systems of two equations with two unknown values—δ_{j*} and δ_j.

Following the first iteration idea we will search now for the number j^{**} of that additional corrector for which $q_j^{(2)}$ has the smallest value. So that after the second iteration we will have fixed the numbers j^* and j^{**} of two optimum correctors.

This kind of iteration procedures go ahead, adding one new corrector at every step, until the sum of the corrected orbit deviations becomes less than a given small value ε . Furthermore the method finds the smallest number of correctors satisfying this condition.

We use extensivly MICADO correction algorithm for simulation of COSY orbit correction due to the fact that this algorithm is implemented in the computer program MAD and that we use MAD as a basic tool for COSY lattice development.

Fig. 25-27 show the results of the simulation of MICADO correction.

10.5 Hereward— Bacconier's Method

In this correction method the following goal function is introduced[28-31] :

$$q = \gamma\sum_{i=1}^{N}\eta_i^2+(1-\gamma)\sum_{j=1}^{K}\delta_j^{c2}\rightarrow\min \tag{10.5.1}$$

In (10.5.1), γ is a parameter, $0<\gamma<1$.

The first sum in (10.5.1) minimizes the orbit deviations in the BPMs, the second one restricts the strengths of the correctors, limiting in this way the influence of the high harmonics of the correction. We saw that from the readings in N BPMs the amplitudes of the first N/2 orbit harmonics can be calculated. These N/2 orbit harmonics are compensated by the corresponding harmonics of the correction. The higher harmonics of the correction remain uncompensated. As they distort the orbit additionally it is useful to restrict their influence.

The optimum value of the parameter γ is determined either experimentally or by computer simulations.

One can write:

$$q = \gamma\sum_{i=1}^{N}\left(\sum_{j=1}^{K}a_{ij}\delta_j^c+\eta_i^{(B+g)}\right)^2+(1-\gamma)\sum_{j=1}^{K}\delta_j^{c2} \tag{10.5.2}$$

The necessary conditions for q to have a minimum is:

$$\frac{\partial q}{\partial\delta_j^c} = 2\gamma\sum_{i=1}^{N}a_{ij}\sum_{p=1}^{K}(a_{ip}\delta_p^c+\eta_i^{(B+g)})+2\,(1-\gamma)\delta_p^c = 0 \qquad j=1,2,\ldots,k \tag{10.5.3}$$

This can be written in matrix form:

$$(\gamma A^TA+(1-\gamma)E)\vec{\delta}^{\,c} = -\gamma A^T\vec{\eta}^{(B+g)} \tag{10.5.4}$$

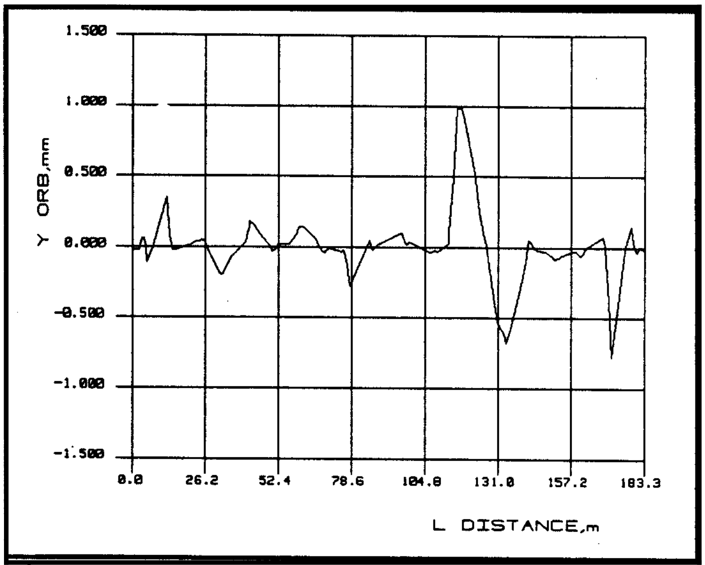

Figure 27.MICADO correction of COSY vertical orbit.

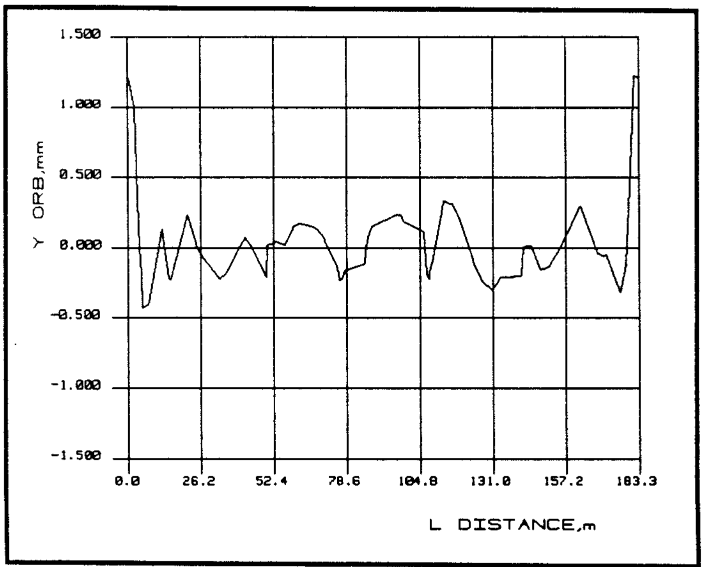

Figure 28. Bacconier's correction of COSY vertical orbit

Fig. 28 shows the results of the simulation of COSY vertical orbit correction by the means of Hereward-Bacconier's method.

10.6 DINAM Orbit Correction Algorithm

Algorithms described above strive to compensate orbit deviations in the points where BPMs are situated by the means of some number of orbit correctors. As a result of the orbit correction, the corrected orbit will have approximately zero deviations in the BPMs. However, between the monitors the corrected orbit will have non-zero deviations. During the computer simulation we noticed that in some particular error distributions the deviations of the corrected orbit in some points are out of control. In general it is important to correct the orbit over the whole accelerator ring and not only in the BPMs.

Emphasizing this fact, we will choose the criterion of correction quality as a functional[32]:

$$q = \frac{1}{2\pi}\int_0^{2\pi}\eta^2(\varphi)\,d\varphi \tag{10.6.1}$$

But the orbit $\eta(\phi)$is a rendom function of the generalized azimuth.This requires to improve the criterion (10.6.1) teking the mathematical expectation of the functional:

$$q = M\left(\frac{1}{2\pi}\int_0^{2\pi}\eta^2(\varphi)\,d\varphi\right) \tag{10.6.2}$$

(10.6.2) is the final form of the correction quality criterion in the DINAM algorithm.

One can write:

$$\frac{1}{\pi}\int_0^{2\pi}\eta^2(\varphi)\delta\varphi = \frac{u_0}{2}+\sum_{k=1}^{\infty}(u_k^2+v_k^2) =$$
$$\left[\frac{u_0^{(B+g)^2}}{2}+\sum_{k=1}^{\infty}\left(u_k^{(B+g)^2}+v_k^{(B+g)^2}\right)\right]+$$
$$\left[u_0^{(B+g)}u_0^{Bc}+\sum_{k=1}^{\infty}\left(2u_k^{(B+g)}u_k^{Bc}+2v_k^{(B+g)}v_k^{Bc}\right)\right]+ \qquad (10.6.3)$$
$$\left[\frac{u_0^{Bc^2}}{2}+\sum_{k=1}^{\infty}\left(u_k^{Bc^2}+v_k^{Bc^2}\right)\right] = \Sigma_1+\Sigma_2+\Sigma_3$$

In (10.6.3) $u_{k1}v_k$ are the Fourier coefficients of the orbit; $u_k^{(B+g)}$ and $v_k^{(B+g)}$ being those caused by the dipole and the quadrupole errors and u_k^{Bc} and v_k^{Bc} being those caused by the correctors.

Let us have 2N Beam position monitors, M—dipoles, L—quadrupoles, and K—correcting dipoles. As a result of the orbit measurement by BPMs, we shall know the orbit distortions in 2N points. However, the total number of the perturbations (M+L) is, as a rule, much larger than the number of BPMs. Therefore, we cannot solve (3.9) about the perturbations. From this system of equations only 2N perturbations can be expressed by the readings in BPMs and other perturbations. In other words, we have a case of correction with uncertainty.

Let η_i, $i=1,2,...,2N$ be the orbit distortions in BPMs. Then we can write:

$$\eta_i = \frac{u_0}{2}+\sum_{k=1}^{\infty}(u_k\cos k\varphi_i+v_k\sin k\varphi_i \quad)_{(i=1,2,...,2N)} \qquad (10.6.4)$$

From these 2N equations, the first N Fourier Coefficients u_0, u_1, . . . , u_N, . . . ,$v_{(n-1)}$ can be expressed by the orbit distortions η_i and higher orbit harmonics. Assuming that BPMs are placed uniformly along the accelerator ring, the following relations can be deduced from (10.6.4):

$$u_0 = U_0-2\sum_{j=1}^{\infty}u_{2Nj} = U_0-S_0$$
$$u_k = U_k-\sum_{j=1}^{\infty}(u_{2Nj-k}+u_{2Nj+k}) = U_k-S_k \qquad (10.6.5)$$
$$v_k = V_k-\sum_{j=1}^{\infty}(-v_{2Nj-k}+v_{2Nj+k}) = V_k-R_k$$

where—

$$
\begin{aligned}
U_0 &= \frac{1}{N}\sum_{i=1}^{2N} \eta_i \\
U_k &= \frac{1}{N}\sum_{i=1}^{2N} \eta_i \cos k\varphi_i; \quad (k=1,2,\dots,N) \\
V_k &= \frac{1}{N}\sum_{i=1}^{2N} \eta_i \sin k\varphi_i; \quad (k=1,2,\dots,(n-1))
\end{aligned}
\tag{10.6.6}
$$

are Bessel's coefficients— Appendix 3.

Making use of the relations (10.6.5) one can write for the sums in (10.6.3):

$$
\begin{aligned}
\Sigma_1 = &\left[\frac{U_0^2}{2} + \sum_{k=1}^{n-1}(U_k^2+V_k^2) + \frac{U_N^2}{2}\right] + \\
&\left[-U_0S_0 + \sum_{k=1}^{N-1}(-2U_kS_k - 2V_kR_k) - U_NS_N\right] + \\
&\left[\frac{S_0^2}{2} + \sum_{k=1}^{N-1}(S_k^2+R_k^2) + S_N^2 - \frac{U_N^2}{4} + V_N^{(B+g)^2} + \right. \\
&\left.\sum_{k=N+1}^{\infty}\left(u_k^{(B+g)^2} + v_k^{(B+g)^2}\right)\right] = \Sigma_a + \Sigma_b + \Sigma_c
\end{aligned}
\tag{10.6.7}
$$

$$
\begin{aligned}
\Sigma_2 = &\left[U_0u_0^{Bc} + 2\sum_{k=1}^{n-1}(U_ku_k^{Bc} + V_kv_k^{Bc}) + U_Nu_N^{Bc}\right] + \\
&\left[2v_N^{B+g}v_N^{Bc} - u_0^{Bc}S_0 - 2\sum_{k=1}^{n-1}(u_k^{Bc}S_k + v_k^{Bc}R_k) - 2u_N^{Bc}S_N\right] + \\
&\left[2\sum_{k=N+1}^{\infty}(u_k^{(B+g)}u_k^{Bc} + v_k^{(B+g)}v_k^{Bc}\right] = \\
&\Sigma_d + \Sigma_e + \Sigma_f
\end{aligned}
\tag{10.6.8}
$$

Using the fact that the higher orbit harmonics are statistically independent and have a zero mathematical expectation we obtain that:

$$M\left(\sum_d\right) = M\left(\sum_e\right) = M\left(\sum_f\right) = 0 \tag{10.6.9}$$

Using the Fourier expansion (3.13) and the reactions (3.14) between the orbit and the perturbation harmonics one can also obtain that:

$$M\left(\sum_c\right) = 4\sum_{k=N+1}^{\infty}\left(\frac{Q^2}{Q^2-k^2}\right)^2 D \tag{10.6.10}$$

where D is the variance of the perturbation harmonics:

$$D = D(f_k) = D(g_k) \tag{10.6.11}$$

Because the correcting dipoles are short compared to the accelerator circumference, one can reduce integrals in the expressions for correctors Fourier harmonics to sums and write:

$$\sum_d = \sum_{p=1}^{2N}\sum_{q=1}^{K} A_{pq}\eta_p\delta_q^{Bc} \tag{10.6.12}$$

where:

$$\begin{aligned} A_{pq} &= \frac{1}{N}\left(c_0 + 2\sum_{k=1}^{n-1} c_k \cos k(\varphi_p - \varphi_q) + c_N \cos N\varphi_p \cos N\varphi_q\right) \\ c_k &= \frac{2Q\sin\pi Q}{\pi^2(Q^2-k^2)} \end{aligned} \tag{10.6.13}$$

In the same way one can prove that:

$$\sum_3 = \sum_{q=1}^{k}\sum_{r=1}^{k} B_{qr}\delta_q^{Bc}\delta_r^{Bc} \tag{10.6.14}$$

where:

$$B_{qr} = \frac{c_o^2}{2} + \sum_{k=1}^{\infty} c_k^2 \cos K(\varphi_q - \varphi_r) =$$
$$\cos Q|\varphi_q - \varphi_r| + \frac{\sin \pi Q}{\pi Q}\cos(\pi - |\varphi_q - \varphi_r|)Q -$$
$$\frac{|\varphi_q - \varphi_r| \sin \pi Q}{\pi} \sin(\pi - |\varphi_q - \varphi_r|)Q \tag{10.6.15}$$

Finally in the applied harmonic analysis it is proved that:

$$\Sigma_a = \frac{1}{N}\sum_{i=1}^{2N} \eta_i^2 \tag{10.6.16}$$

Summarizing all the above results for the quality criterion (10.6.2) we get:

$$2q = \frac{1}{N}\sum_{i=1}^{2N} \eta_i^2 + \sum_{p=1}^{2N}\sum_{q=1}^{k} A_{pq}\eta_p \delta_q^{Bc} +$$
$$\sum_{q=1}^{k}\sum_{r=1}^{k} B_{qr}\delta_q^{Bc}\delta_r^{Bc} + 4\sum_{k=n+1}^{\infty}\left(\frac{Q^2}{Q^2-k^2}\right)D \tag{10.6.17}$$

The coefficients A_{pq} and B_{qr} are given by formulae (10.6.13) and (10.6.15) respectively. In these formulae, φ_p are the azimuths of the BPMs and φ_q and φ_r are the azimuths of the correcting dipoles.

The strengths of the correcting dipoles are determined by the condition for a minimum of q to occur:

$$2\sum_{p=1}^{k} B_{sp}\delta_p^{Bc} = -\sum_{p=1}^{2N} A_{ps}\eta_p \qquad (s=1,2,\ldots,k) \tag{10.6.18}$$

Introducing matrices $A=\{A_{ij}\}$ and $B=\{B_{ij}\}$ and the vectors of the corrections $\vec{\delta}^{Bc}$ and BPMs readings $\vec{\eta}$ eq. (10.6.18) can be written in the following matrix form:

$$2B\vec{\delta}^{Bc} = -A^T\vec{\eta} \tag{10.6.19}$$

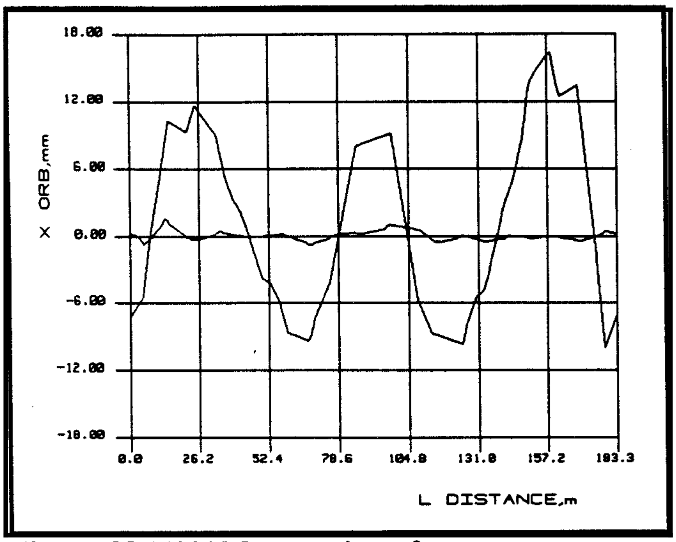

Figure 29.DINAM correction of the COSY horizontal orbit compared with the initial orbit.

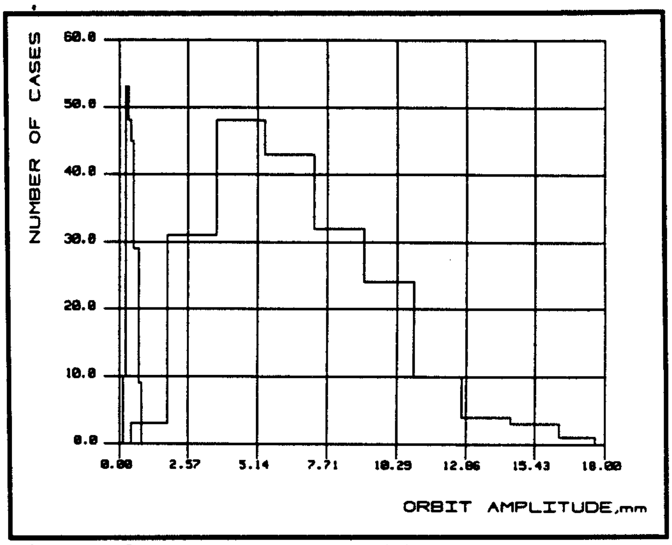

Figure 30.Max.deviations of COSY hor.orbit before and after DINAM corrections.

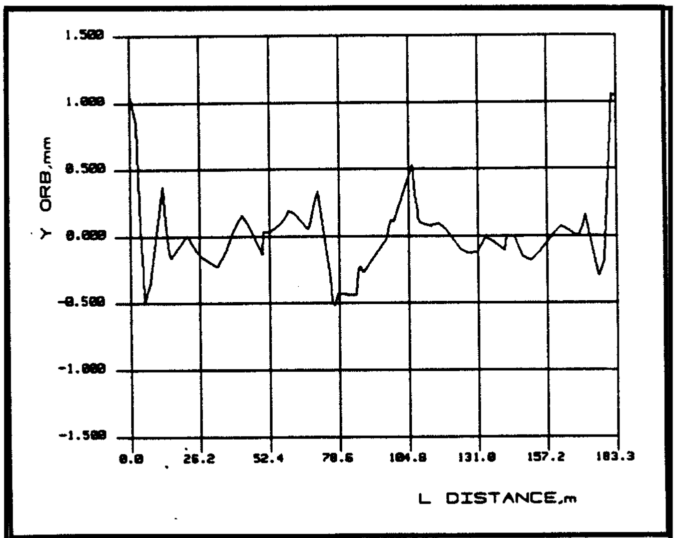

Figure 31.DINAM correction of COSY vertical orbit.

Let us introduce the matrix:

$$R = -\frac{1}{2}B^{-1}A^{T} \qquad \textbf{(10.6.20)}$$

The matrix R depends only on the azimuths of the BPMs and on the correctors and for the given accelerator it can be calculated prior to the correction. Then the required strengths of the correcting dipoles will be determined by the matrix expression:

$$\vec{\delta}^{Bc} = R\cdot\vec{\eta} \qquad \textbf{(10.6.21)}$$

So the algorithm is relatively fast. The computer simulations showed that it works reliably and is free from the undesirable effects mentioned in the beginning of this part.

Some results of the computer simulations of COSY orbit by DINAM algorithm are shown on Fig. 29-31.

11. COSY Horizontal Orbit Correction with Coupled Back-Leg Windings

As we have already pointed out, besides separate steering magnets in the telescopes back-leg correcting windings in the bending dipoles will be wed for COSY horizontal correction.

The back-leg windings, however, change the main magnet coils inductivity. This can cause an instability in the main magnet power supply operation. To avoid such troubles all the back-leg windings have to be coupled in a way the members of any pair to be fed by equal and opposite currents. In other words, the back-leg windings should be grouped in pairs, each pair producing two equal and opposite correcting kicks.

Obviously, the magnets taking part in such a pair have to be separated by a phase advance approximately equal to π. In this case, the two equal and opposite correcting kicks will affect the orbit in one and the same direction. Taking into account for simplicity only the main

$\bar{k}\approx Q$ harmonic of the correction we can write(see(3.13)):

$$f_{k} = \frac{1}{\pi Q}\epsilon_{+}\left(\sqrt{\beta_{+}}\cos\bar{k}\varphi_{+} - \sqrt{\beta_{-}}\cos\bar{k}\varphi_{-}\right) \qquad \textbf{(11.1)}$$

In the optimum case: $\mu_- = \mu_+ + \pi;\ \varphi_- = \varphi_+ + \dfrac{\pi}{Q}$:

$$f_{\bar{k}} \approx \frac{1}{\pi Q}\epsilon_+ \cos\bar{k}\varphi_+ (\sqrt{\beta_+} + \sqrt{\beta_-}) \qquad (11.2)$$

and analogously:

$$g_{\bar{k}} \approx \frac{1}{\pi Q}\epsilon_+ \sin\bar{k}\varphi_- (\sqrt{\beta_+} + \sqrt{\beta_-}) \qquad (11.3)$$

It is most straightforward to generalize the LSQ correction algorithm for the case of coupled back-leg windings.

Let us rearrange correctors in a special way, bringing uncoupled correctors $\epsilon_0$as first,following by the first members of these pairs ϵ_+ and finally the second members of these pairs ϵ_-. So we have for the corrector kicks vector:

$$\vec{\epsilon} = (\ \vec{\epsilon}_0 |\ \vec{\epsilon}_+ |\ \vec{\epsilon}_- |\ ) \qquad (11.4)$$

with $\vec{\epsilon}_+ = -\vec{\epsilon}_-$.

According to (3.9) we have:

$$\vec{\eta}^{\,c} = A\ \vec{\epsilon}^{\,c} \qquad (11.5)$$

where:

$$A_{ij} = -\frac{\sqrt{\beta_j}}{2\sin\pi Q}\cos Q(\varphi_i + \pi - \varphi_j) \qquad (11.6)$$

Let's divide the matrix A to three submatrices A_0, A_+, and A_- corresponding to the three vectors $\vec{\epsilon}_0, \vec{\epsilon}_+, \vec{\epsilon}_-$:

$$A = \{\ A_0 \mid A_+ \mid A_-\ \}$$

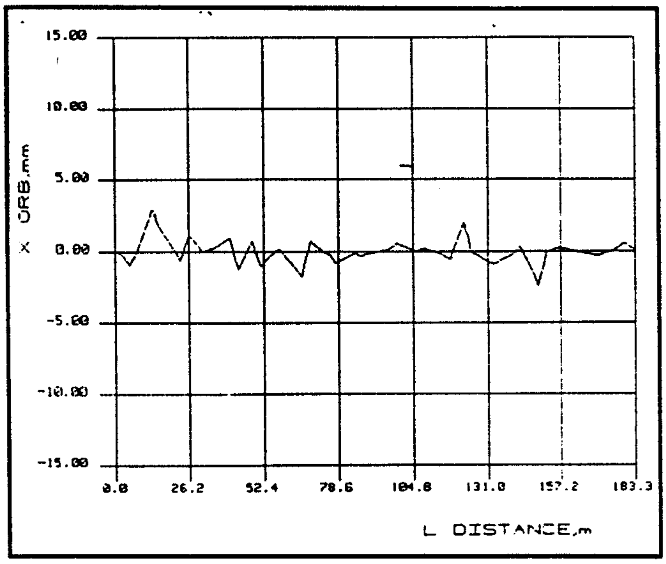

Figure 32. Correction of COSY horizontal closed orbit using coupled back-leg correcting windings.Q_x=Q_z=3.38.

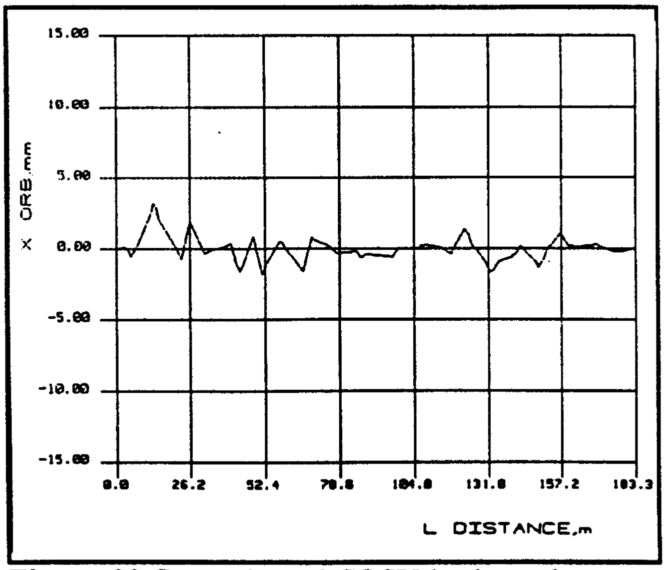

Figure 33. Correction of COSY horizontal closed orbit using coupled back-leg correcting windings.Q_x=Q_z=4.25.

i.e.

$$\vec{\eta}^{\,c} = A_0\vec{e}_0 + A_+\vec{e}_+ + A_-\vec{e}_+ = A_0\vec{e}_0 + (A_+ - A_-)\vec{e}_+ \tag{11.8}$$

We can introduce the reduced correctors kicks vector:

$$\vec{e}_* = (\ \vec{e}_0 \mid \vec{e}_+\ ) \tag{11.9}$$

and reduced matrix:

$$A_* = \{A_0 | A_+ - A_-\} \tag{11.10}$$

The following matrix relation exists for the reduced quantities:

$$\vec{\eta}^{\,c} = A_*\vec{e}_* \tag{11.11}$$

As in the pure LSQ method we will minimize the goal function:

$$q = \sum_{i=1}^{N} \eta_i^2 = \vec{\eta}^{\,T}\vec{\eta} = (\vec{\eta}^{(B+g)} + \vec{\eta}^{\,c})^T(\vec{\eta}^{(B+g)} + \vec{\eta}^{\,c}) \rightarrow \min \tag{11.12}$$

It follows from (11.12) and (11.11) that:

$$\vec{e}_{*opt} = -(A_*^T A_*)^{-1} A_*^T \vec{\eta}^{(B+g)} \tag{11.13}$$

Then using (11.9) and (11.4) we are able to reconstruct all correctors kicks.
The results of the simulation of the COSY horizontal orbit correction applying coupled back-leg windings are shown in fig. 32. In keeping with the above considerations, the back-leg windings in the magnets 1 and 7, 2 and 8 and so on were jointed in couples.

12. Other Correction Methods

We shall only mention here some other suggested methods for orbit correction: eigen vectors method[11], analytical approach[34] and the use of ℓ_p norms[35].

13.COSY Orbit Correction with Separate Dipole Correctors

We have studied also the case of using separate dipole correcting magnets of C-type insted of the back-leg windings in the main dipoles.The layout of the correctors and beam position monitors for this case is given in Table 2.

In order to estimate the necessary correctors strengths and the expected maximum orbit deviations we simulated the orbit correction for 200 machines with diferent distributions of the random errors.

According to this statistics we can expect a corrected orbit with maximum deviation(on the whole ring,not only in the beam position monitors) less than 2mm.

In 95% of the cases the necessary correctors strengths were less than 1 mrad;the maximum received
kicks were 1.7 mrad.

14. Notes About COSY Orbit Correction

Summarizing the results from the COSY orbit simulation given above, we can say that maximum closed orbit deviations less than 18 mm. in the horizontal and 14 mm in the vertical planes can be expected.

We studied especially $Q_x = Q_z = 3.38$ working point. The correctors and pick-up monitors layout was shown in Table 1. All separate correctors and only 12 of all the 24 back-leg correcting windings in the main magnets have been used.

The maximum correctors kicks have reached 1.2 mrad for the horizontal and 0.8 mrad for the vertical plane. We studied also the possibility of using coupled back-leg windings as orbit correctors. We jointed the back-leg windings in 1st and 7th, 2nd and 8th, and so on magnets in pairs, so that the members of each pair to produce equal in magnitude and opposite in sign kicks. We proved that the orbit correction is still possible with about 3 mm maximum deviation of the corrected orbit. The
necessary maximum correctors kicks in this case are bigger and have reached 1.5 mrad.

We studied the case of using separate dipole correctors (insted of the back-leg windings in the main dipoles) for the horizontal orbit correction.Orbit amplitudes less than 2mm can be expected after the correction in this case.

The most general considerations about the orbit correction shows that the BPMs and the correctors should be placed near the points with $\beta =$ max, as both BPM sensitivity and correctors impact upon the orbit are proportional to $\sqrt{\beta}$, see (3.3, 3.11). Both have to be as regular distributed along the accelerator ring as possible. Following the beam-bump algorithm, we can see that about $K \approx 4Q$ correctors are necessary. In the case of COSY cooler synchrotron, this most general recommendations have been taken into account as far as this has been possible.

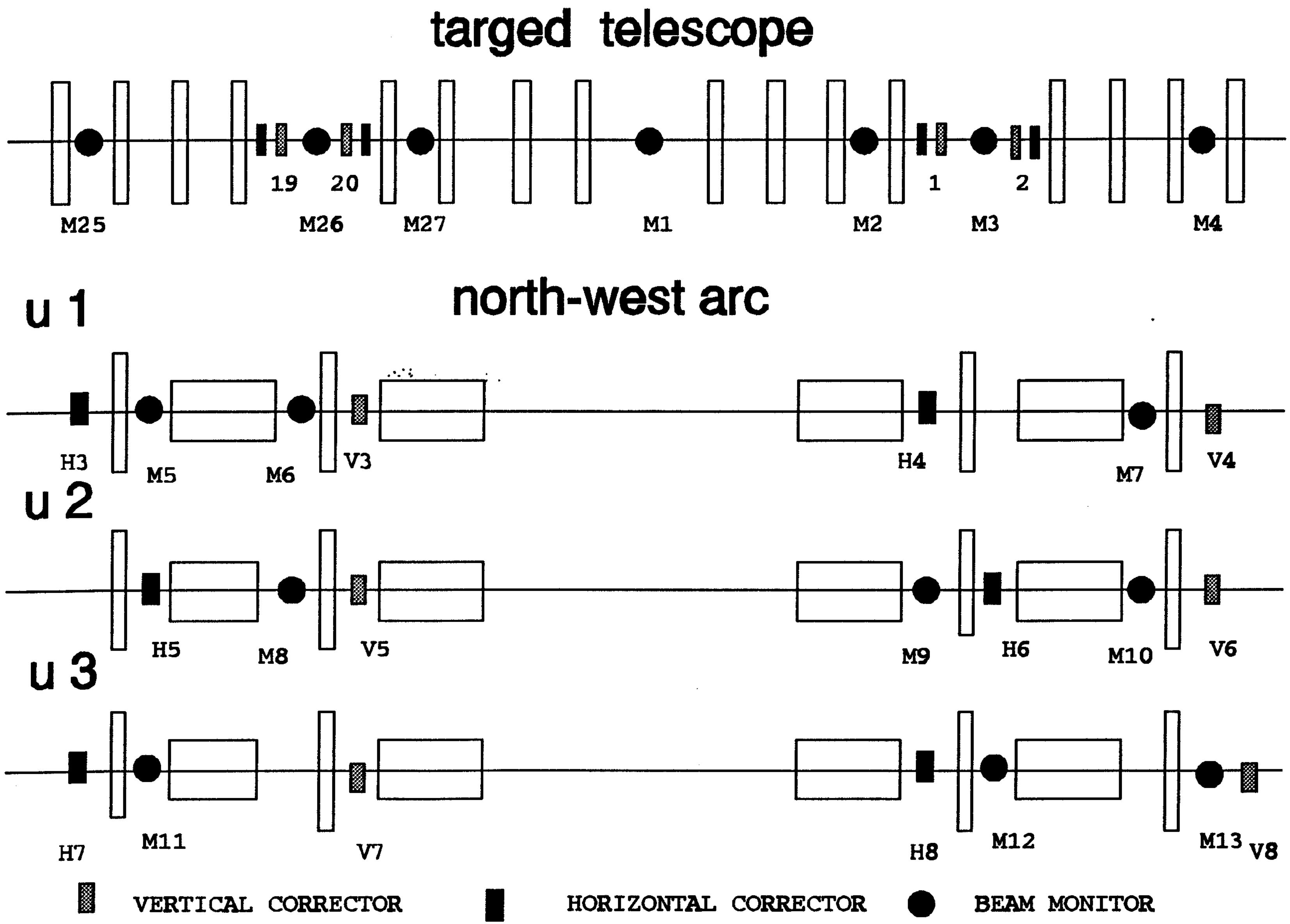
targed telescope
M25
19
M26
20
M27
M1
M2
1
M3
2
M4
north-west arc
u 1
H3
M5
M6
V3
H4
M7
V4
u 2
H5
M8
V5
M9
H6
M10
V6
u 3
H7
M11
V7
H8
M12
M13
V8
VERTICAL CORRECTOR
HORIZONTAL CORRECTOR
BEAM MONITOR

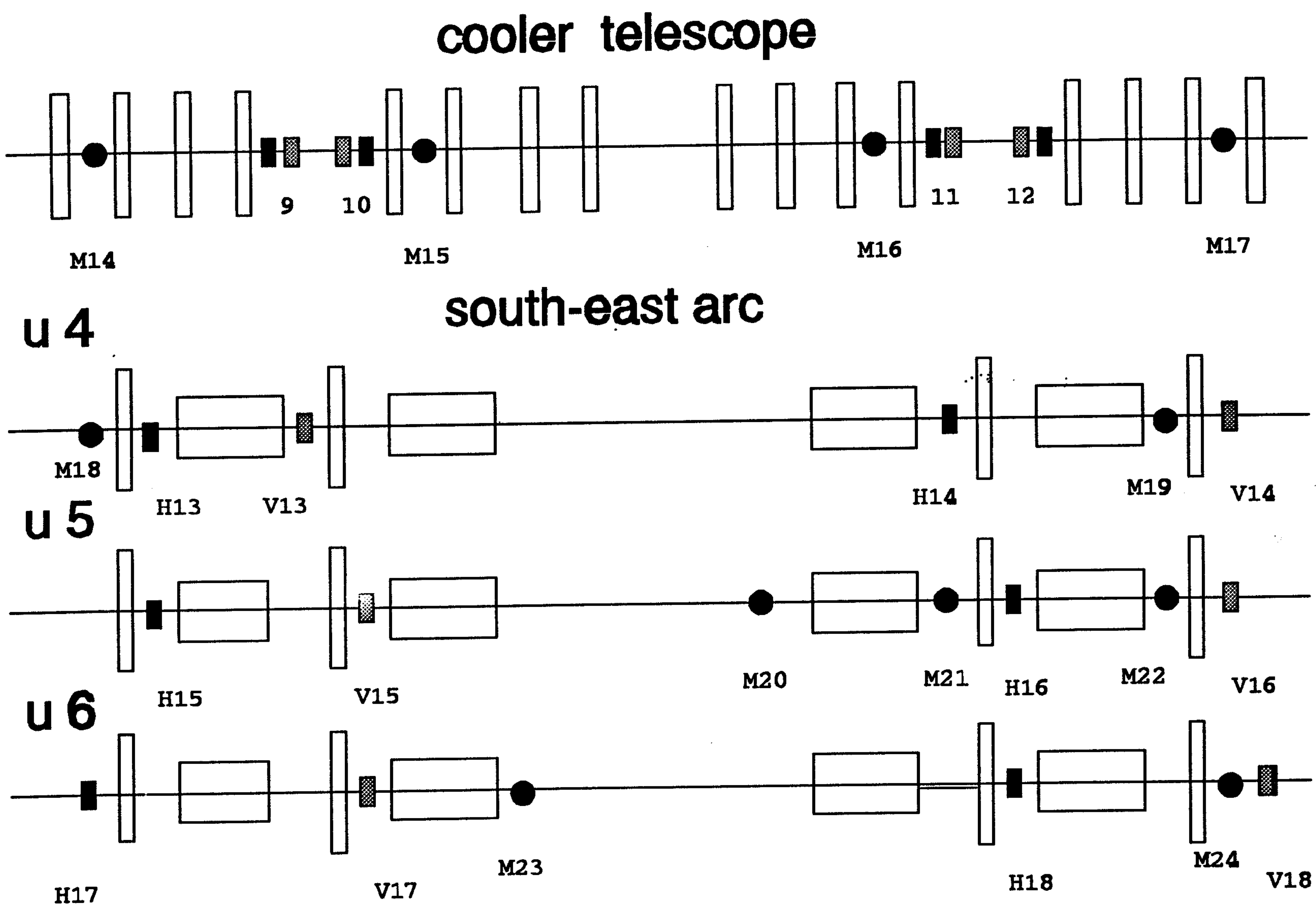

TABLE 2. NEW ARRANGEMENT OF COSY DIPOLE CORRECTORS AND BPMs.

According to paragraph 4, we can expect errors which are constant during the cycle, proportional to the main magnetic field and appearing only in high fields. Correctors strengths have to follow this time behavior:

$$\Delta B_c \sim A + Bi(t) + C(t) \tag{13.1}$$

where:
i(t) is the current in the main magnet,
C(t) is a function describing the saturation.

The most important characteristics of each orbit correction is the correction quality[32] defined as:

$$K_c = \frac{\sigma(\eta_{corr})}{\sigma(\eta)} \tag{13.2}$$

In[32] an analytical estimation of the correction quality is made. Assuming a completely regular structure with 2N beam position monitors and the same number of correctors, k=2N one can deduce that:

$$K_c^2 = K_0^2 + \frac{\sigma^2(\epsilon_\eta)}{\sigma^2(\eta)} + a\frac{\sigma^2(\epsilon_\delta)}{\sigma^2(\eta)} \tag{13.3}$$

In (13.3) K_0 is the correction quality without any errors in monitor readings and in correcting currents; the second member describes the influence of the errors in BPMs readings; the third member describes the influence of the errors in the correcting fields (currents). The above formula describes the intuitively clear fact that due to the errors in BPMs and correctors, it is not worthwhile to use an enormous number of monitors and correctors and to reduce in this way K_0 close to zero; in such a case the prevalent will be the last two members in (13.3), caused by the errors.

In (13.3) $\sigma(\epsilon_\eta)$ are the rms errors for the normalized orbit —(3.2) and $\sigma(\epsilon_\delta)$ are the rms errors for the generalized corrector strengths—(3.11). a is a constant, depending only on the number of correctors— K=2N:

$$a = N\left(\frac{c_o^2}{2} + \sum_{k=1}^{N-1} c_k^2 + \frac{c_N^2}{2}\right) \tag{13.4}$$

where—

$$c_k = \frac{2Q\sin\pi Q}{\pi(Q^2-k^2)} \tag{13.5}$$

For the COSY synchrotron, errors less than 0.1 mm in the BPMs and less than 0.1% in the correctors are expected[39].
These relatively low error limits lead to—

$$K_c^2 \approx K_0^2 + 3.10^{-4} \tag{13.6}$$

which show a low disturbance of the orbit correction by the errors.

14. Acknowledgement

The author thanks Drs. D. Prasulin, K. Bongardt, H. Stockhorst and R. Wagner from COSY theory group for the fruitful discussions.

He is glad to express especially his gratitude to Dr. S. Martin for a large number of stimulating discussions and useful advice.

Appendix 1

Some Basic COSY Parameters

Energy range:	40 Mev-2.5 GeV (protons)
maximum beam intensity:	2.10^{11} ppp
circumference:	184 m
betatron frequency:	
Q_x, Q_z:	3.38, 3.38
magnetic structure:	seperated function, 6 periods FDDF or DFFD
Acceptance:	$A_x = 180\ \pi$ mm mrad $A_z = 35\ \pi$ mm mrad
bending magnets:	
— No	24
— bending radius	s= 7m
— maximum field	1.67T
arc quadrupoles:	
— No	24
— effective length	0.29m
— maximum gradient	7.5T/m
telescope quadrupoles:	
— No	32
— effective length	0.29m
— maximum gradient	7.65T/m
RF system:	
— harmonic number	h=1
— frequency range	0.462-1.572MHz
— energy gain per turn:	1.3 KeV
vacuum:	$< 10^{-10}$ hPa

Appendix 2

Orbit Interpolation

It is always useful for the orbit deviations between BPMs to be known. But as a rule, BPMs are not uniformly distributed along the accelerator circumference. So we are to use one of the interpolation formulae with non-regular set of data points[35,36]:

A. Language interpolation:

$$\eta(\varphi) \approx \frac{(\varphi-\varphi_2)(\varphi-\varphi_3)...(\varphi-\varphi_n)}{(\varphi_1-\varphi_2)(\varphi_1-\varphi_3)...(\varphi_1-\varphi_n)}\eta_1+...+ \frac{(\varphi-\varphi_1)(\varphi-\varphi_2)...(\varphi-\varphi_{n-1})}{(\varphi_{n-1}-\varphi_1)(\varphi_{n-1}-\varphi_2)...(\varphi_{n-1}-\varphi_{n-2})}\eta_n \qquad \text{(A2.1)}$$

B. Trigonometrical interpolation:

$$\eta(\varphi) \approx \sum_{k=0}^{2n} \eta_k t_{kn}(\varphi) \qquad \text{(A2.2)}$$

where:

$$t_{kn}(\varphi) = \frac{\sin\frac{\varphi-\varphi_1}{2}...\sin\frac{\varphi-\varphi_{k-1}}{2}\sin\frac{\varphi-\varphi_{k+1}}{2}...\sin\frac{\varphi-\varphi_{2n}}{2}}{\sin\frac{\varphi_k-\varphi_1}{2}...\sin\frac{\varphi-k-\varphi_{k-1}}{2}\sin\frac{\varphi_k-\varphi_{k+1}}{2}...\sin\frac{\varphi_k-\varphi_{2n}}{2}} \qquad \text{(A2.3)}$$

C. Cubic Spline Interpolation:

This is a piecewise interpolation which keeps continuous the function and its first and second derivatives[35]. In every subinterval $[\varphi_i, \varphi_{i+1}]$ the interpolant s (φ) is a cubic polinomial $S_i(\phi)$and:

i)

$$s_i(\varphi_1) = \eta_i; \quad s_i(\varphi_{i+1}) = \eta_{i+1} \qquad \text{(A2.4)}$$

ii)

$$s'_{i-1}(\varphi_i) = s'_i(\varphi_i) \tag{A2.5}$$

iii)

$$s''_{i-1}(\varphi_i) = s''_i(\varphi_i) \tag{A2.6}$$

Two additional conditions are set in the terminal points of the considered interval, $\varphi = 0$ *and* $\varphi = 2\pi$ in our case:

a) for the so-called free cubic spline:

$$s''_1(0) = s''_n(2\pi) = 0 \tag{A2.7}$$

b) for the so-called clamped cubic spline:

$$\begin{aligned} s'_1(0) &= \eta'_0 \\ s'_n(2\pi) &= \eta'_n = \eta'_0 \end{aligned} \tag{A2.8}$$

Appendix 3

Some Useful Formulae of the Applied Harmonic Analysis

Let:

$$\varphi_0(x),\varphi_1(x),\dots,\varphi_n(x) \qquad \text{(A3.1)}$$

be a system of orthonormal functions in the interval [a,b].

In the harmonic analysis[37,38] we approximate a given function f(x) by a linear combination of the functions (A3.1):

$$f(x) \sim \sum_{k=0}^{n} c_u \varphi_k(x) \qquad \text{(A3.2)}$$

so that:

$$\frac{1}{(b-a)}\int_a^b [f(x)-\sum_{k=0}^{n} c_k \varphi_k(x)]^2 dx \rightarrow \min \qquad \text{(A3.3)}$$

It is proved that the minimum of (A3.3) occurs for the so-called Fourier coefficients:

$$c_k = \int_a^b f(x)\varphi_k(x)dx \qquad \text{(A3.4)}$$

In the applied harmonic analysis we do not know the whole function f(x) but only its values y_i in some points $x_i,\ y_i = f(x_i), i = 1,2,\dots,p$. As in the harmonic analysis we will aim to approximate the function f(x) with a linear combination of ortonormal functions (A3.2), but because we know only "p" values of f(x) the criterion of the approximation should be modified to:

$$\sum_{i=1}^{p}\left[y_i-\sum_{k=0}^{n} c_k' \varphi_k(x_i)\right]^2 \rightarrow \min \qquad \text{(A3.5)}$$

The most popular is the case of a system of trigonometrical functions:
1, sin x, cos x, sin 2x, cos 2x, . . .
in the $[-\pi, \pi]$ interval.

This case (A3.4) leads to the well known formulae:

$$A_k = \frac{1}{\pi}\int_{-\pi}^{\pi} f(x)\cos kx dx$$
$$B_k = \frac{1}{\pi}\int_{-\pi}^{\pi} f(x)\sin kx dx \qquad \text{(A3.7)}$$

where we have changed for simplicity the notations C_k by A_k, B_k for the cos— and sin—coefficients respectively.

It is proved that in the limit $n \to \infty$ the representation (A3.2) becomes exact— the well-known Fourier series:

$$f(x) = \frac{A_0}{2} + \sum_{k+1}^{\infty} (A_k \cos x + B_k \sin kx) \qquad \text{(A3.8)}$$

In the case of the applied harmonic analysis the system of trigonometrical functions (A3.6) and the approximation criterion (A3.5) lead to the so-called Bessel's co-efficients.

$$A_0' = \frac{2}{p}\sum_{i-1}^{p} y_i$$
$$A_k' = \frac{2}{p}\sum_{i-1}^{p} y_i \cos kx_i \qquad \text{(A3.5)}$$
$$B_k' = \frac{2}{p}\sum_{i-1}^{p} y_i \sin kx_i$$

It is proved that the following relations between the Bessel's coefficients A_k', B_k' and the Fourier coefficients A_k, B_k exists:

$$A_k' = A_k + A_{p-k} + A_{p+k} + \dots \qquad \text{(A3.10)}$$
$$B_k' = B_k - B_{p-k} + B_{p+k} - \dots$$

So one can regard at Bessel's coefficients A'_k, B'_k as an approximation of the Fourier coefficients A_k, B_k in the case when we know only the meanings y_i of the function f(x) under consideration in some points x_i, $i=1,2,\ldots,p$.

Some better approximation for the Fourier coefficients have been deduced by A.A. Eagle. Let $y_0, y_1, \ldots y_{2v-1}$ be the meanings of the function f(x) in 2v points $x_0, x_1, \ldots, x_{2v-1}$.

a) broken-line approximation:

$$\begin{aligned} A'_k &= -\frac{v}{\pi^2 k^2}\sum_{i=0}^{2v-1} \Delta^2 y_i \cos kx_i \\ B'_k &= -\frac{v}{\pi^2 k^2}\sum_{i=0}^{2v-1} \Delta^2 y_i \sin kx_i \end{aligned} \tag{A3.11}$$

where:

$$\Delta^2 y_i = y_{i+1} - 2y_i + y_{i-1}$$

b) paraboles approximation:

$$\begin{aligned} A'_k &= \frac{v}{2\pi^2 k^2}\sum_{i=1}^{v} \Delta^4 y_{2i} \cos kx_{2i} + \frac{v}{\pi^2 K^3}\sum_{i=1}^{v} (\Delta^2 y_{2i+1} - \Delta^2 y_{2i-1}) \sin kx_{2i} \\ B'_k &= \frac{v}{2\pi^2 k^2}\sum_{i=1}^{v} \Delta^4 y_{2i} \sin kx_{2i} - \frac{v}{\pi^2 k^3}\sum_{i=1}^{v} (\Delta^2 y_{2i+1} - \Delta^2 y_{2i-1}) \cos kx_{2i} \end{aligned} \tag{A3.12}$$

where—

$$\Delta^4 y_{2i} = y_{2i+2} - 4y_{2i+1} + 6y_{2i} - 4y_{2i-1} + y_{2i-2}$$

c) cubic paraboles approximation:

$$\begin{aligned} A'_k &= \frac{3v^3}{k^4 \pi^4}\sum_{i=0}^{2v-1} \Delta^4 y_i \cos kx_i - \frac{v^2}{k^3 \pi^2}\sum_{i=0}^{2v} (\Delta^2 y_{i+1} - \Delta^2 y_{i-1}) \sin kx_i \\ B'_k &= \frac{3v^3}{k^4 \pi^4}\sum_{i=0}^{2v-1} \Delta^4 y_i \sin kx_i - \frac{v^2}{n^3 \pi^2}\sum_{i=0}^{2v} (\Delta^2 y_{i+1} - \Delta^2 y_{i-1}) \cos kx_i \end{aligned} \tag{A3.13}$$

References

1.U.Pfister,R.Theenhaus.The COSY-Julich Project.2nd European Particle Accelerators Conference,Nice,1990.
2.K.Kilian,R.Maier,S.Martin,U.Pfister.Cooler Synchrotron COSY-Julich.User Guide.Forschungszentrum Julich,1990.
3.A.A.Kolomensky,A.N.Lebedev.Theory of Cyclic Accelerators.North-Holland Publishing Co.,Amsterdam,1966.
4.H.Bruck.Accelerateurs Circulaires de Particules.Presses Universitaires de France,Paris,1966.
5.F.Christoph Iselin,J.Niederer.The MAD Program.Version 6.User's Reference Manual.CERN/LEP-TH/87-33,Geneva,1987.
6.K.Bongardt,D.Dinev,S.Martin,P.F.Meads,D.Prasuhn,H.Stockhorst,R.Wagner.The COSY Lattice.2nd European Particle Accelerators Conference,Nice,1990.
7.P.Strolin.Concerning Two-Dimentional Probability Distributions of Closed Orbit Distortions.CERN-ISR-TH/68-4,1968.
8.R.Gluckstern.Distribution of the Maximum Orbit Distortion for Randomly Distributed Misalignments.Particle Accelerators,V.8,1978,pp.203-208.
9.L.Resegotti.Provisions for the Correction of Closed Orbit Distortions in the ISR.CERN-ISR-MAG/68-30,1968.
10.B.Autin,R.J.Bryant.Closed Orbit Manipulation and Correction in the CERN ISR.CERN/ISR-MA/71-36,1971.
11.A.Ando,K.Endo.Correction of Closed Orbit at Injection in Alternating-Gradient Synchrotron.KEK-75-4,1975.
12.G.Guignard.The Closed Orbit Measurements as a Diagnostic Tool for Localization and Correction of Misalignments in the ISR.CERN-ISR-BOM/80-21,1980.
13.D.Brandt,A.Verdier.Exhaustive Search of Field Defect Compensation.EPAC,Rome,1988,pp.654-656.
14.H.Kugler et all.Closed Orbit Distortions and Their Corrections in the 600 MeV Electron-Positron Accumulator at LEP.EPAC,Rome,1988,pp.758-760.
15.J.L.Warren,P.J.Channell.New Method for Inverting the Closed Orbit Distortion Problem.IEEE Trans.Nucl.Sci.,NS-30,No 4,1983.
16.P.J.Averill.IEEE Trans.Nucl.Sci.,June,1965.
17.C.Bovet,K.H.Reich.CERN/SI/Int.DL/69-3,Geneva,1969.
18.G.Holtey.CERN/Lab.2-D1-PA/Int.73-3,Geneva,1973.
19.S.Peggs.Some Aspects of Machine Physics in the Cornell Electron Storage Ring.Ph.D.Thesis,Cornell,1981.
20.V.Paxson,S.Peggs,L.Schachinger.Iteractive First Turn and Global Closed Orbit Correction in the SSC.EPAC,Rome,1988,pp.824-826.
21.L.Burnod,E.D'Amico.New Methods to Correct On-line the Closed Orbit in a Synchrotron Accelerators with Variable Focusing Configuration.IEEE Trans.Nucl.Sci.,V.NS-30,No 4,1983.
22.G.Guignard,Y.Marti.PETROC User's Guide.CERN/ISR-BOM-TH/81-32,1981.
23.G.Guignard,Y.Marti.Numerical Simulation of Orbit Correction in Large Electron Rings.CERN/LEP-TH/83-50,1983.
24.E.Bozoki.The ORBCOR Program.CERN/PS/PSR/85-57,1985.
25.M.Martini,L.Rinolfi.Closed Orbit Correction of the CERN Antiproton Collector

Ring,EPAC,Rome,1988,pp.842-844.
26.T.Risselada.An Improved Vertion of yhe Orbit Correction Program ORBCOR.CERN/PS/87-90,1987.
27.B.Autin,Y.Marty.Closed Orbit Correction of A.G.Machines Using a Small Number of Magnets.CERN-ISR-MA/73-17,Geneva,1973.
28.Y.Bacconier.Contribution a l'etude de l'orbite ferme.CERN,65-35,Geneva,1965.
29.G.Guignard.CERN/SI/Int.Dl/70-1,Geneva,1970.
30.G.Guignard.CERN/SI/Int.Dl/70-2,Geneva,1970.
31.G.Guignard.Effects des chamos magnetique perturbateur d'un synchrotron sur l'orbite fermee et les oscillations betatroniques,ansi que leur compensation.CERN/70-24,Geneva,1970.
32.P.Vasilev,D.Dinev.Correction Algorithm of a Closed Orbit in Synchrotrons.Bulg.J.Phys.,V.12,No 5,1985.
33.J.Miles.Prelimenary Note on Closed Orbit Correction in the l_p Norms.CERN-SPS/AOP/Note 83-3,Geneva,1983.
34.J.P.Maidment,C.W.Planner.An Analytic Method for Closed Orbit Correction in High Energy Synchrotrons.Nuclear Instruments and Methods,1971.
35.I.Jacques,C.Judd.Numerical Analysis.Chapman and Hall,London,1987.
36.C.Gerald,P.Wheatley.Applied Numerical Analysis.Addison-Wesley Publishing Company,1989.
37.P.W.Hamming.Numerical Methods for Scientists and Engineers.New York,McGraw-Hill,1962.
38.R.W.Hamming.Introduction to Applied Numerical Analysis.New York,1971.
39.R.Maier et all.Non-Beam Disturbing Diagnostics at COSY-Julich.2nd European Particle Accelerators Conference,Nice,1990.